A Synergistic Workspace for Human Consciousness Revealed by Integrated Information Decomposition

Andrea I. Luppi[1,2]*, Pedro A.M. Mediano[3], Fernando E. Rosas[4,5,6], Judith Allanson[1,7], John D. Pickard[1,8,9], Robin L. Carhart-Harris[4,10], Guy B. Williams[1,8], Michael M Craig[1,2], Paola Finoia[1], Adrian M. Owen[11], Lorina Naci[12], David K. Menon[2,8], Daniel Bor[3], & Emmanuel A. Stamatakis[2]

[1]Department of Clinical Neurosciences, University of Cambridge, Cambridge, CB2 0QQ, United Kingdom.
[2]University Division of Anaesthesia, School of Clinical Medicine, University of Cambridge, Cambridge, CB2 0QQ, United Kingdom.
[3]Department of Psychology, University of Cambridge, Cambridge, CB2 3EB, United Kingdom.
[4]Center for Psychedelic Research, Department of Brain Science, Imperial College London, London W12 0NN, United Kingdom.
[5]Center for Complexity Science, Imperial College London, London SW7 2AZ, United Kingdom.
[6]Data Science Institute, Imperial College London, London SW7 2AZ, United Kingdom.
[7]Department of Neurosciences, Cambridge University Hospitals NHS Foundation, Addenbrooke's Hospital, Hills Rd, CB2 0SP, Cambridge, United Kingdom
[8]Wolfson Brain Imaging Centre, University of Cambridge, Cambridge, CB2 0QQ, United Kingdom.
[9]Division of Neurosurgery, School of Clinical Medicine, University of Cambridge, Addenbrooke's Hospital, Hills Rd, CB2 0SP, Cambridge, United Kingdom
[10]Psychedelics Division - Neuroscape, Department of Neurology, University of California, San Francisco, CA 94143
[11]Department of Psychology and Department of Physiology and Pharmacology, The Brain and Mind Institute, N6A 5B7 University of Western Ontario, London, Ontario, Canada.
[12]Trinity College Institute of Neuroscience, School of Psychology, Lloyd Building, Trinity College Dublin, Dublin 2, Ireland.
*Correspondence: al857@cam.ac.uk

Abstract

A central goal of neuroscience is to understand how the brain orchestrates information from multiple input streams into a unified conscious experience. Here, we address two fundamental questions: how is the human information-processing architecture functionally organised, and how does its organisation support consciousness? We combine network science and a rigorous information-theoretic notion of synergy to delineate a "synergistic global workspace", comprising gateway regions that gather synergistic information from specialised modules across the brain. This information is then integrated within the workspace and widely distributed via broadcaster regions. Through functional MRI analysis, we show that gateway regions of the synergistic workspace correspond to the brain's default mode network, whereas broadcasters coincide with the executive control network. Demonstrating the empirical relevance of our proposed architecture for neural information processing, we show that loss of consciousness due to general anaesthesia or disorders of consciousness corresponds to a diminished ability of the synergistic workspace to integrate information, which is restored upon recovery. Thus, loss of consciousness coincides with a breakdown of information integration within the synergistic workspace of the human brain. This work contributes to conceptual and empirical reconciliation between two prominent scientific theories of consciousness, the Global Neuronal Workspace and Integrated Information Theory. Taken together, this work provides a new perspective on the role of prominent resting-state networks within the human information-processing architecture, while also advancing our understanding of how the human brain supports consciousness through the synergistic integration of information.

Keywords: synergy, global workspace, integrated information, brain networks, anaesthesia, disorders of consciousness

Introduction

Humans and other vertebrates rely on a centralised nervous system to process information from the environment, obtained from a wide array of sensory sources. Information from different sensory sources must eventually be combined - and integrated - with the organism's memories and goals, in order to guide adaptive behaviour effectively [1]. However, understanding how the brain's information-processing architecture enables the integration of information remains a key open challenge in neuroscience [2,3]. Theoretical and empirical work in cognitive neuroscience indicates that information processed in parallel by domain-specific sensory modules needs to be integrated within a multimodal "central executive" [4]. Indeed, recent work has identified subsets of regions that are consistently recruited across a variety of tasks [5–7], situated at the convergence of multiple anatomical, functional, and neurochemical hierarchies in the brain [8–20].

Prominent theories in cognitive and computational neuroscience have also proposed that global integration of information from diverse sources plays a fundamental role in relation to human consciousness [21,22]. The influential Global Neuronal Workspace Theory (GNWT) focuses on the process by which specific neural information becomes available for conscious access, as occurring through the global integration induced by a "global workspace" [23–26]. Within the workspace, relevant information from different sources is integrated and subsequently broadcasted back to the entire brain, in order to inform further processing and achieve "experiential integration" of distributed cortical modules into a coherent whole [24,25,27]. Thus, the global workspace is attributed both the role of integrator, and the role of orchestrator of cognitive function. Also highlighting the importance of integration, the prominent Integrated Information Theory (IIT) [21,28,29] posits that the degree of consciousness in a system is determined by its "integrated information": the amount of intrinsic information generated by the dynamics of the system considered as a whole, over and above the information generated by the dynamics of its individual constituent parts [21,28–30]. Thus, this notion of integrated information corresponds to the extent to which "the whole is greater than the sum of its parts" [31].

Therefore, leading theoretical accounts of consciousness converge on this point: consciousness critically depends on the capability for global integration across a network of differentiated modules. Despite agreeing on the fundamental importance of information integration [32], these theories differ on its specific role and corresponding neural mechanisms. In contrast to GNWT's account, whereby integration is viewed as a necessary - but not sufficient - prerequisite step on the way to broadcasting and consciousness, IIT proposes a more fundamental identity between consciousness and the integration of information, but without specifying a formal architecture for this process: that is, according to IIT any system that integrates information will thereby be conscious, regardless of its specific organisation [31]. Seen under this light, it becomes apparent that IIT and GWT are actually addressing different aspects of consciousness, and their views of integration are different but potentially complementary.

Crucially, our ability to make sense of any information-processing architecture is limited by our understanding of the information that is being processed. An elegant account of information in distributed systems - such as the human brain - is provided by the framework of Partial Information Decomposition (PID) [33] which demonstrates that not all information is equal. Two sources can possess information about a given target that is either unique (each source provides independent information), redundant (the same information is provided by both sources) or synergistic (complementary information, a higher-order kind of information that is available only when both sources are considered together). As an example, humans have two sources of visual information about the world: two eyes. The information that is lost when one eye is closed is called the "unique information" of that source - information that cannot be obtained from the remaining eye. The information that one still has when one eye

is closed is called “redundant information” - because it is information that is carried equally by both sources. This provides robustness: you can still see even after losing one eye. However, losing one eye also deprives you of stereoscopic information about depth. This information does not come from either eye alone: you need both, in order to perceive the third dimension. Therefore, this is called the “synergistic information” between the sources - the extra advantage that is derived from combining them.

There is growing appreciation that higher-order information dynamics may play a key role in the distributed information-processing architecture of the brain [34–37]. By applying a recent generalisation of PID to timeseries data – known as Integrated Information Decomposition [38] – we developed an information-resolved approach to decompose the information carried by brain dynamics and their intrinsic fluctuations [39]. Going beyond traditional measures of statistical association (“functional connectivity”), the information-resolved framework revealed that different regions of the human brain predominantly rely on different kinds of information for their interactions with other regions. Through this approach, we identified a “synergistic core” of brain regions supporting higher-level cognitive functions in the human brain through the synergistic integration of information [39]. We also observed that a synergy-based measure of emergent dynamics is disrupted in patients suffering from chronic disorders of consciousness [40]. Building on these findings, it is natural to ask whether this synergistic core could correspond to the brain’s global workspace. Furthermore, given that the views on information integration put forward by GNWT and IIT are potentially complementary, an important challenge to move the field forward is to leverage both accounts into a unified architecture that could explain empirical effects observed in neuroimaging data.

Therefore, this work sets out to address two fundamental questions of contemporary neuroscience:

1. How is the cognitive architecture of the human brain functionally organised, from an information-processing standpoint? Specifically, what brain regions does it involve, and what are the roles of the two kinds of information integration proposed by GNWT and IIT within this architecture?
2. How are these information-processing roles related to human consciousness?

To address these questions, and provide an information-resolved view of human consciousness, here we study three resting-state fMRI datasets: (i) N=100 subjects from the Human Connectome Project; (ii) N=15 healthy volunteers who were scanned before and after general anaesthesia with the intravenous propofol as well as during post-anaesthetic recovery [41]; (iii) N=22 patients suffering from chronic disorders of consciousness (DOC) as a result of severe brain injury [41].

Results

Adopting an information-resolved view, we propose to divide the information-processing stream within the human brain in three key stages: (i) gathering of information from multiple distinct modules into a workspace; (ii) integration of the gathered information within the workspace; and (iii) global information broadcasting to the rest of the brain. Furthermore, we propose that while all workspace regions are involved in stage (ii), they are differentially involved in stages (i) and (iii).

The existence of a synergistic workspace and these three processing stages can be seen as emerging from a trade-off between performance and robustness that is inherent to distributed systems. Theoretical work in cognitive science [26] and the field of distributed signal

processing [42,43] has long recognised the computational benefits of combining multiple distinct processing streams. However, having a single source of inputs to and outputs from the workspace introduces what is known as a "single point of failure," which can lead to catastrophic failure in case of damage or malfunction [44]. Therefore, a natural solution is to have not a single but multiple units dedicated to gathering and broadcasting information, respectively, thereby forming a workspace that can be in charge of synthesising the results of peripheral processing [45].

Pertaining to Stage (ii), we previously identified which regions of the human brain are predominantly synergistic, and thus are most reliant on combining information from other brain regions [39]. The key signature of workspace regions is to have a high prevalence of synergistic (compared to redundant) connections, and therefore the synergy-rich regions that we discovered are ideally poised as GNW candidates. Here, we consider the architecture of the global workspace more broadly, and combine Integrated Information Decomposition with graph-theoretical principles to bring insights about processing stages (i) and (iii) (Figure 1). We term this proposal the "Synergy-Φ-Redundancy" neurocognitive architecture (SAPHIRE) (Figure 1).

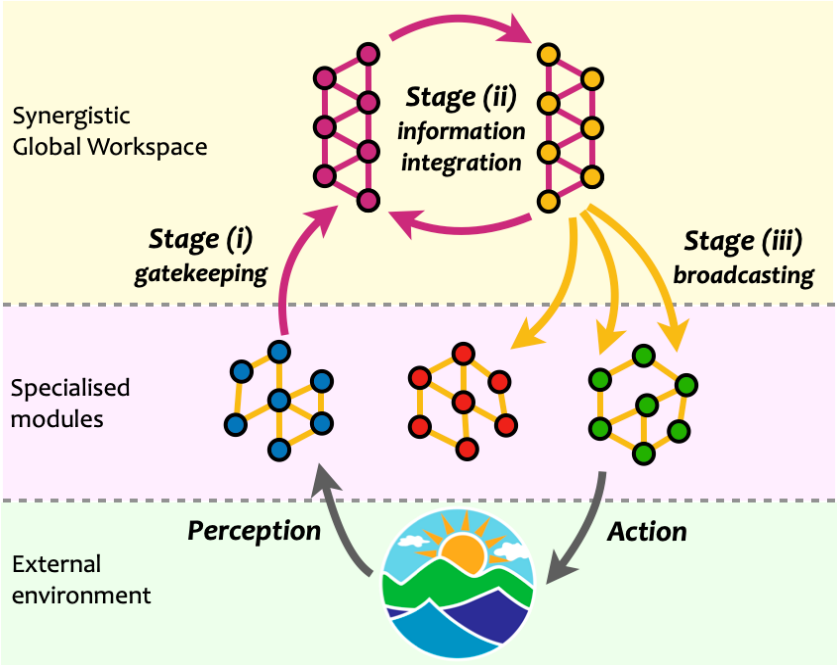

Figure 1. Schematic of the proposed SAPHIRE neurocognitive architecture. Below, specialised modules characterised by robust redundant interactions process information about the environment. Information is then collected by workspace gateways through synergistic interactions [Step (i)]; synergistic interactions integrate information within the synergistic global workspace [Step (ii)]; workspace broadcasters spread the integrated information back to the specialised modules, through redundant interactions [Step (iii)], for further processing and to guide behaviour. Orange connections represent redundant interactions, and violet connections represent synergistic interactions. Grey connections represent interactions between the system and its environment.

We note that brain regions through which information gains access to the workspace should exhibit synergistic connections that are widely distributed across the brain, as - by definition - the workspace gathers and synthesises information from a multiplicity of diverse brain modules. Thus, we postulate that regions that mediate the access to the synergistic workspace are connected with multiple modules within networks of synergistic interactions,

synthesising incoming inputs from diverse sources [46,47]. We refer to such regions as *gateways* (Figure 1, violet nodes). In contrast, the process of broadcasting information corresponds to disseminating multiple copies of the same information from the workspace to many functionally adjacent brain regions. Therefore, broadcaster regions also have connections with many different modules, but of non-synergistic, redundant connections: "redundancy" accounts for the fact that multiple copies of the same information are being distributed. These regions are designated as *broadcasters* (Figure 1, orange nodes).

One approach to operationalise these ideas is by leveraging well-established graph-theoretical tools. Here, we propose to assess the diversity of intermodular connections using the *participation coefficient* [48] which captures to what extent a given node connects to modules beyond its own (Methods). Note that this is different from the node *strength,* which captures a region's total amount of connectivity, and which we used to identify which regions belong to the synergistic workspace (see Methods and [39]); the participation coefficient instead quantifies the diversity of modules that a region is connected to. Therefore, gateways are identified as brain regions that (a) belong to the workspace, and (b) have a highly-ranked participation coefficient in terms of synergistic connections. Conversely, broadcasters are global workspace regions that have a higher participation coefficient rank over redundant connections.

To explore these hypotheses, we computed synergistic and redundant interactions between 454 cortical and subcortical brain regions [49,50] based on resting-state functional MRI data from 100 subjects of the Human Connectome Project [39]. We then subdivided the brain into the well-established resting-state networks identified by Yeo and colleagues [51] plus an additional subcortical module [52]. Based on this partition into modules, we identified gateways and broadcasters by comparing the participation coefficients of synergistic versus redundant connections, for brain regions belonging to the synergistic workspace previously identified.

Intriguingly, our results reveal that gateways reside primarily in the brain's default mode network (Figure 2B, violet). In contrast, broadcasters are mainly located in the executive control network, especially lateral prefrontal cortex (Figure 2B, orange). Remarkably, the latter results are in line with Global Neuronal Workspace Theory, which consistently identifies lateral prefrontal cortex as a major broadcaster of information [24,53].

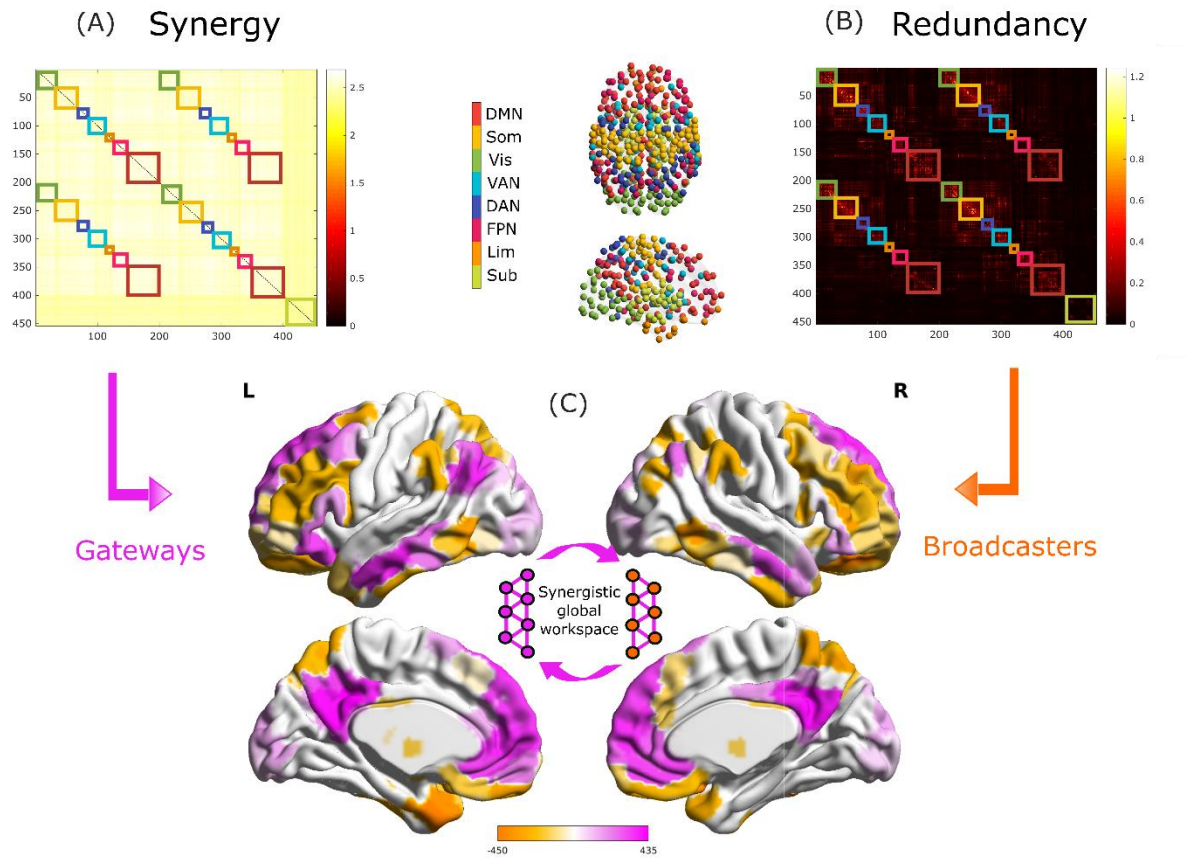

Figure 2. Gateways and broadcaster regions identified by their network connectivity profiles. (A) Group-average matrices of synergistic interactions between regions of the 454-ROI augmented Schaefer atlas (39, 43). (B) Group-average matrices of redundant interactions. We highlighted modular allegiance to the canonical resting-state networks by using the colour scheme shown in between A and B. (C) Regions are identified as gateways (violet) or broadcasters (orange) based on the difference between rank of participation coefficient for synergy and redundancy, (only shown for brain regions identified as belonging to the synergistic global workspace). Violet indicates synergy rank > redundancy rank, corresponding to workspace regions that combine information of many brain modules (gateways); orange indicates the opposite, identifying workspace regions that broadcast information to many modules. Inset: illustration of the synergistic workspace. Legend: DMN, default mode network. Som, somatomotor network. Vis, visual network. VAN, ventral attention network. DAN, dorsal attention network. FPN, fronto-parietal control network. Lim, limbic network. Sub, subcortical network (comprised of 54 regions of the Tian 2020 atlas [52]). These results were also replicated using an alternative parcellation with 232 cortical and subcortical nodes (SI Figure 1).

Information decomposition identifies a synergistic core supporting human consciousness

Having introduced a taxonomy within the synergistic global workspace based on the distinct information-processing roles of different brain regions, we then sought to investigate their role in supporting human consciousness. Given the importance attributed to integration of information by both GNWT and IIT, we expected to observe reductions in integrated information within the areas of the synergistic workspace associated with loss of consciousness. Furthermore, we also reasoned that any brain regions that are specifically involved in supporting consciousness should “track” the presence of consciousness: the reductions should occur regardless of how loss of consciousness came about, and they should be restored when consciousness is regained.

We tested these hypotheses with resting-state fMRI from 15 healthy volunteers who were scanned before, during, and after anaesthesia with the intravenous agent propofol, as well

as 22 patients with chronic disorders of consciousness (DOC) [41]. Resting-state fMRI data were parcellated into 400 cortical and 54 subcortical brain regions. Building on the IIT literature, which provides a formal definition of integrated information, we assessed integration corresponding to conscious activity via two alternative metrics: the well-known whole-minus-sum Φ measure introduced by Balduzzi and Tononi [31], and the "revised Φ" (Φ_R) measure recently introduced by Mediano, Rosas and colleagues [38] (Methods and SI Figure 2). Being demonstrably non-negative, this revised measure overcomes a major conceptual limitation of the original formulation of integrated information [38].

For each subject, we computed the integrated information between each pair of BOLD signal timeseries, resulting in a 454-by-454 matrix of integrated information between brain regions. Treating this matrix as an (undirected) network enabled us to study consciousness-related changes in integrated information across conditions, which were analysed using the Network Based Statistic correction for multiple comparisons [54]. Importantly, since we are interested in changes that are shared between the DOC and propofol datasets, we computed edge-level statistics using a composite null hypothesis test designed to detect such shared effects (Methods).

Analysis based on Φ_R revealed a widespread reorganisation of integrated information throughout the brain when comparing awake volunteers against DOC patients, with both increases and decreases being observed ($p < 0.001$; Figure 3A). Likewise, propofol anaesthesia was also characterised by significant changes in integrated information between brain regions, both when compared with pre-anaesthetic wakefulness ($p < 0.001$; Figure 3B) and post-anaesthetic recovery ($p < 0.001$; Figure 3C).

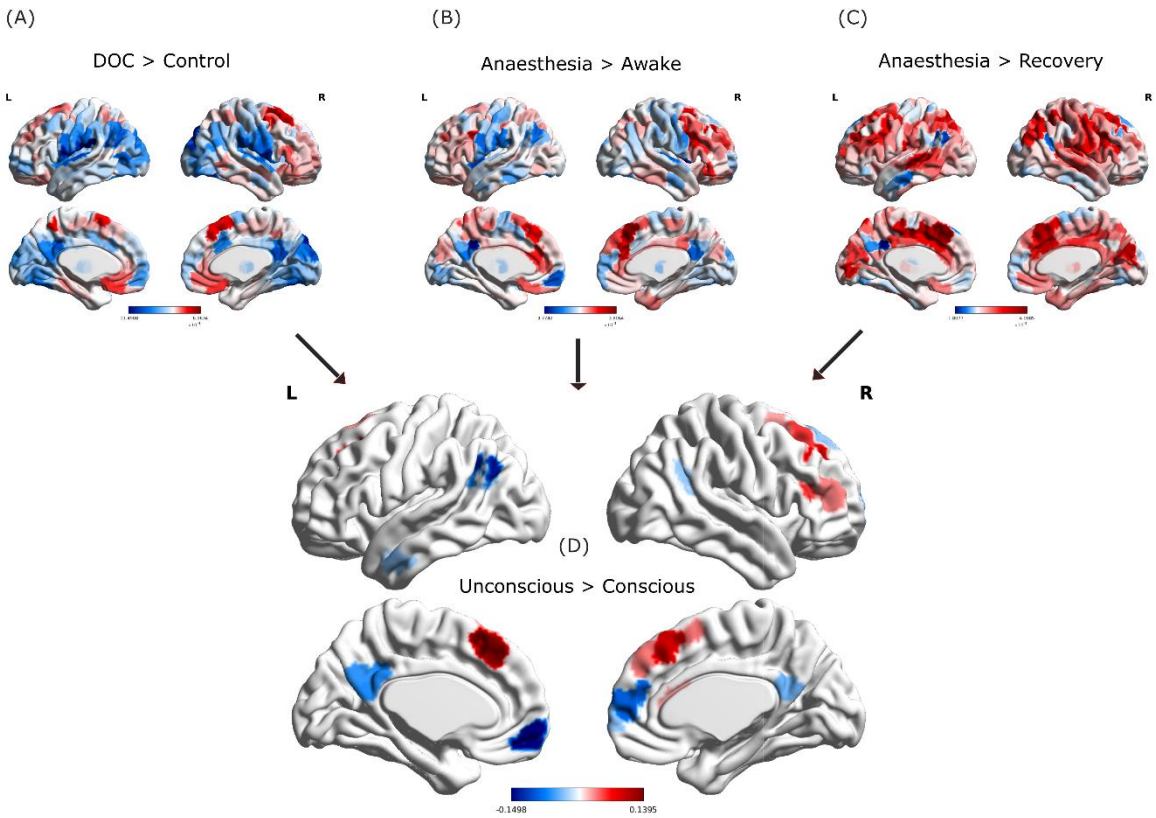

Figure 3. Loss of consciousness induces similar reorganisation of cortical integrated information across anaesthesia and disorders of consciousness. Top: Brain regions exhibiting overall NBS-corrected increases (red) and decreases (blue) in integrated information exchange when consciousness is lost. (A) DOC patients

minus awake healthy volunteers; (B), propofol anaesthesia minus pre-induction wakefulness; (C) propofol-anaesthesia minus post-anaesthetic recovery. (D) Overlaps between the three contrasts in (A-C), showing increases and decreases that are common across anaesthesia and disorders of consciousness.

Our analysis identified a number of the Φ_R connections that were reduced when consciousness was lost due to both anaesthesia and brain injury, and were restored during post-anaesthetic recovery - as we had hypothesised (Figure 3D). Remarkably, almost all regions showing consistent decreases in Φ_R when consciousness was lost were members of the global synergistic workspace, and specifically located in the default mode network (bilateral precuneus and medial prefrontal cortex) - and bilateral inferior parietal cortex – although left temporal cortices were also involved (Figure 3D). Additionally, some connections exhibited increases in Φ_R during loss of consciousness, and were restored upon recovery (Figure 3D), including areas in frontal cortex - especially lateral prefrontal cortex. Nevertheless, the overall balance was in favour of reduced integrated information: sum of F-scores associated with significant edges = -25.37 (SI Figure 3). This was in contrast with the analysis based on the original formulation of Φ introduced by Balduzzi and Tononi [31], which did not identify any reductions in integrated information that were common across anaesthesia and disorders of consciousness, instead only identifying common increases (SI Figure 4A).

Having identified the subset of brain regions that are reliably associated with supporting human consciousness in terms of their integrated information, the last step of our analysis was to leverage the architecture proposed above to understand their role in the information processing stream within the brain. Since IIT predicts that loss of consciousness corresponds to reductions in integrated information, we focused on regions exhibiting reliable reductions in Φ_R when consciousness is lost (whether due to anaesthesia or DOC), which were restored upon recovery (shown in blue in Figure 3D).

Remarkably, our whole-brain results show that Φ_R disconnections induced by loss of consciousness play the role of gateway nodes (Figure 3A, violet) rather than broadcaster nodes (Figure 4A, orange) according to our previous identification (see Figure 2B, violet regions). Indeed, all reductions occur specifically within the default mode network (Figure 4B). Thus, these results suggest that loss of consciousness across anaesthesia and disorders of consciousness would correspond to anterior-posterior disconnection - in terms of integrated information - between DMN nodes that act as gateways into the synergistic workspace.

Replication with alternative parcellation

To ensure the robustness of our results to analytic choices, we also replicated them using an alternative cortical parcellation of lower dimensionality: we used the Schaefer scale-200 cortical parcellation [50] complemented with the scale-32 subcortical ROIs from the Tian subcortical atlas [52] (SI Figure 4B). Additionally, we also show that our results are not dependent on the choice of parameters in the NBS analysis, and are replicated using an alternative threshold definition for the connected component (extent rather than intensity) or a more stringent value for the cluster threshold ($F > 12$) (SI Figure 4C-D). Importantly, whereas the increases in Φ_R are not the same across different analytic approaches, reductions of Φ_R in medial prefrontal and posterior cingulate/precuneus are reliably observed, attesting to their robustness.

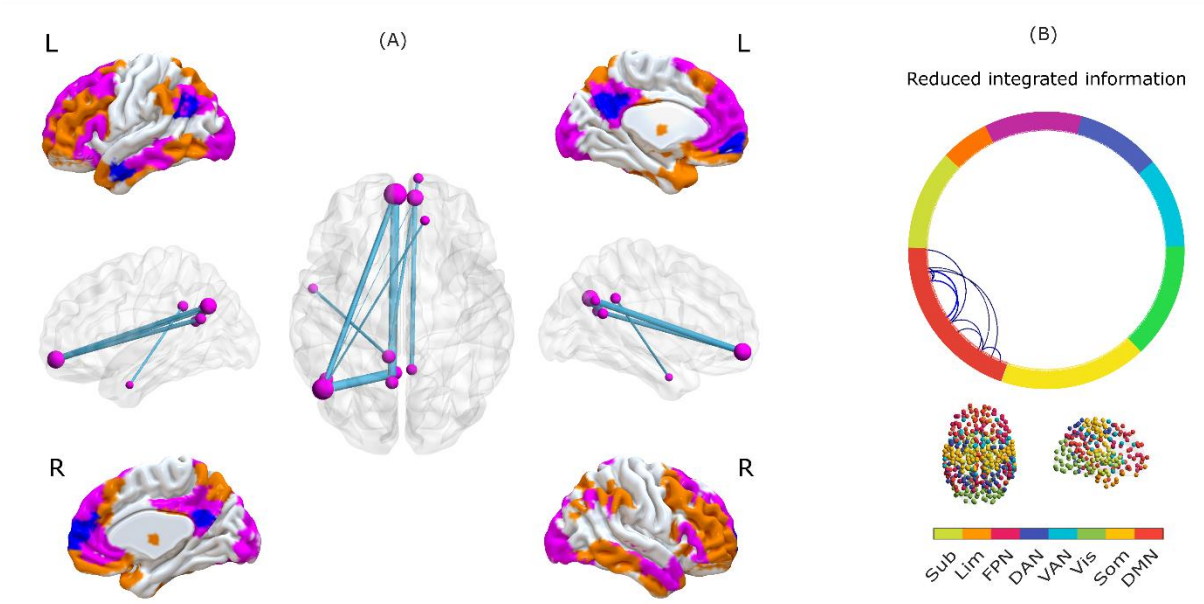

Figure 4. Synergistic core of human consciousness. (A) Surface projections indicate brain regions that play the role of broadcasters (orange) or gateways (violet) in the synergistic workspace, and regions that exhibit an overall significant reduction in integrated information across anaesthesia and disorders of consciousness (blue). Network representation: edges indicate reduced integrated information during both propofol anaesthesia and disorders of consciousness, between gateway (violet) and broadcaster (orange) nodes of the workspace. (B) Circular graph representation of significant reductions in integrated information (Φ_R) between brain regions, observed in all three contrasts, divided into canonical resting-state networks. Legend: DMN, default mode network. Som, somatomotor network. Vis, visual network. VAN, ventral attention network. DAN, dorsal attention network. FPN, fronto-parietal control network. Lim, limbic network. Sub, subcortical network (comprised of 54 regions of the Tian 2020 atlas).

Discussion

Architecture of the synergistic global workspace

This paper proposes a functional architecture for the brain's macroscale information processing flow, which leverages insights from network science and a refined understanding of neural information exchange. The synergy-Φ-redundancy (SAPHIRE) architecture posits the existence of a "synergistic workspace" of brain regions characterised by highly synergistic global interactions, which we previously showed to be composed by prefrontal and parietal cortices that are critical for higher cognitive functions [39]. This workspace is further functionally decomposed by distinguishing gateways, which bring information from localised modules into the workspace, and broadcasters, which disseminate multiple copies of workspace information back to low-level regions.

Remarkably, our results on the HCP dataset show that the proposed operationalisation of gateways and broadcasters corresponds to the distinction between the brain's default mode network and executive control network, respectively. This data-driven identification of workspace gateways and broadcasters with the DMN and FPN provides a new framework to explain well-known functional differences between DMN and FPN, based on their distinct and complementary roles within the brain's synergistic global workspace, which is discussed below.

The fronto-parietal executive control network (FPN) mainly comprises lateral prefrontal and parietal cortices, and it is associated with performance of a variety of complex, cognitively demanding tasks [55–57]. A key component of this network is lateral prefrontal cortex (LPFC). Based on theoretical and empirical evidence, as summarised in a recent review of GNWT [24], this region is posited to play a major role in the global workspace, as a global broadcaster of information. Remarkably, this is precisely the role that our results assigned to LPFC, based on its combined information-theoretic and network properties. These results are also consistent with recent insights from network neuroscience, which indicate that the FPN is ideally poised to steer whole-brain dynamics through novel trajectories, in response to complex task demands [57,58]. Specifically, by broadcasting to the rest of the brain information that has been integrated within the workspace, the FPN may act as global coordinator of subsequent whole-brain dynamics.

On the other hand, the default mode network comprises posterior cingulate and precuneus, medial prefrontal cortex, and inferior parietal cortices [59–61]. This network, whose constituent regions have undergone substantial developments in the course of human evolution [62,63], was found to occupy a crucial position at the convergence of functional gradients of macroscale cortical organization [15,64,65], forming a structural and functional core of the human brain [66–68], in line with its recently observed involvement in cognitive tasks [69–71]. In particular, the DMN is prominently involved in self-referential processing [72,73], and 'mental-time-travel' [74] or episodic memory and future-oriented cognition [75–78]. Its posterior regions in particular, act as relays between the neocortex and the hippocampal memory system [76]. Thus, in terms of both neuroanatomical connectivity and functional engagement, the DMN is uniquely positioned to integrate and contextualise information coming into the synergistic global workspace (e.g. from sensory streams) by combining it with rich information pertaining to one's past experiences and high-level mental models about 'self' and world [65,79–83] - coinciding with the results of the present analysis, which identify DMN nodes as gateways of inputs to the synergistic global workspace.

It is worth noting that the role of the FPN-DMN tandem in supporting consciousness has been suggested by Shanahan's hypothesis of a 'connective core' along the brain's medial axis [84]. While Shanahan's hypotheses were primarily based on structure, in this work we combine novel information-theoretic tools to confirm and expand the connective core hypothesis from a functional, information-processing perspective, in a way that differentiates the multiple roles played by the different regions that together comprise this connective core (Figures 2,4).

Integrated Information Decomposition of human consciousness

After identifying the neuroanatomical-functional mapping of the synergistic workspace in terms of gateways and broadcasters, we sought to identify their role in supporting human consciousness. Considering integrated information as a measure of consciousness, we focused on identifying regions where information integration is reduced when consciousness is lost (regardless of its cause, be it propofol anaesthesia or severe brain injury), and restored upon its recovery. Our results indicate that brain regions exhibiting consciousness-specific reductions in integrated information coincide with major nodes of the synergistic global workspace.

Intriguingly, we found that the main disruptions of information integration were localised in gateway nodes, rather than broadcasters. Thus, loss of consciousness in both anaesthesia and disorders of consciousness could be understood as a breakdown of the entry points to the "synergistic core" (Figure 4), which becomes unable to properly integrate inputs for the workspace. Importantly, the original "whole-minus-sum" Φ introduced by Balduzzi and Tononi [31] did not show consistent reductions during loss of consciousness. Thus, the present

results demonstrate the empirical validity of the "revised" measure, Φ_R, in addition to its theoretical soundness [38]. Since workspace gateway regions coincide with the brain's default mode network, these results are also in line with recent evidence that information content and integrative capacity of the DMN are compromised during loss of consciousness induced by both anaesthesia and severe brain injury [41,85–93], and even COVID-19 [94]. Due to its prominent role in self-referential processing [73], breakdown of DMN connectivity within the synergistic workspace may be seen as a failure to integrate one's self-narrative into the "stream of consciousness", in the words of William James.

This notion is further supported by focusing on reductions of integrated information during anaesthesia compared with wakefulness. In addition to the synergistic core, overall reductions are also observed in a set of thalamic, auditory and somatomotor regions, largely resembling the brain regions that stop responding to sensory (auditory and noxious) stimuli once the brain reaches propofol-induced saturation of EEG slow-wave activity (SWAS [95]). Although there was no EEG data available to confirm this, the doses of propofol employed in the present study are compatible with the doses of propofol at which SWAS has been shown to arise [96], and therefore it is plausible that our participants also reached SWAS and the loss of brain responsiveness it indicates.

Thus, both resting-state integration of information between brain regions, as well as stimulus-evoked responses within each region [95], converge to indicate that propofol disrupts further processing of thalamocortical sensory information – a phenomenon termed "thalamocortical isolation" [95]. We propose that as the thalamus and sensory cortices lose their ability to respond to stimuli, they cease to provide information to the synergistic core of the global workspace, resulting in a disconnection from the external world and presumably loss of consciousness.

These results testify to the power of the Integrated Information Decomposition framework: by identifying the information-theoretic components of integrated information, we have been able to obtain insights about human consciousness that remained elusive with alternative formulations, and could not be captured via standard functional connectivity or related methods. Thus, our findings support the notion that the global workspace is highly relevant for supporting consciousness in the human brain, in line with the proposal that *"[...] unconsciousness is not necessarily a complete suppression of information processing but rather a network dysfunction that could create inhospitable conditions for global information exchange and broadcasting"* [24]. GNWT postulates a key role for the global workspace in supporting consciousness: consistent with this theory, we find that several nodes of the synergistic global workspace become disconnected from each other in terms of integrated information when consciousness is lost, especially between anterior and posterior regions (Figure 4, brain networks). Thus, these are brain regions that (i) belong to the synergistic global workspace; (ii) exhibit overall reductions of integrated information when consciousness is lost; and (iii) are disconnected from other regions of the synergistic workspace when consciousness is lost. The brain regions satisfying these three conditions therefore constitute an interconnected "synergistic core" of workspace regions supporting human consciousness.

Limitations and future directions

in order to obtain high spatial resolution for our identification of workspace regions, here we relied on the BOLD signal from functional MRI, which is an indirect proxy of underlying neuronal activity, with limited temporal resolution. However, we sought to alleviate potential confounds by deconvolving the hemodynamic response function from our data with a dedicated toolbox [97] (Methods), which has been previously applied both in the context of information decomposition [39], as well as anaesthetic-induced loss of consciousness [98], and disorders of consciousness [40].

It is also worth bearing in mind that our measure of integrated information between pairs of regions does not amount to measuring the integrated information of the brain as a whole, as formally specified in the context of Integrated Information Theory [31] - although we do show that the average integrated information between pairs of regions is overall reduced across the whole brain. We also note that our revised measure of integrated information is based on IIT 2.0 [31], due to its computational tractability; as a result, it relies on a conceptually distinct understanding of integrated information from the more recent IIT 3.0 [99] and IIT 4.0 [100] versions. Thus, these limitations should be borne in mind when seeking to interpret the present results in the context of IIT. Indeed, future work may benefit from seeking convergence with recent advances in the characterization of emergence, which is related to integrated information [101–104].

Intriguingly, although we have focused on anaesthetic-induced decreases in integrated information, due to IIT's prediction that this is what should occur during loss of consciousness, our results also indicate concomitant increases of integrated information – possibly reflecting compensatory attempts, although we refrain from further speculation (Figure 3). Interestingly, increases appear to coincide with broadcaster nodes of the synergistic workspace. In particular, even though lateral prefrontal cortices are among the regions most closely associated with the global neuronal workspace in the literature [24,53], our results indicate a paradoxical net increase in lateral prefrontal integrated information during anaesthesia and DOC. We interpret this qualitatively different behaviour as indicating that different subsets of the global workspace may be differentially involved in supporting consciousness.

However, we note that, whereas the decreases in integrated information were robust to the use of different analytic approaches (e.g., use of a different parcellation or different NBS threshold), the increases that we observed were less robust, with no region consistently showing increases in integrated information (SI Figure 4B-D). Nevertheless, both this phenomenon and the meaning of increased integrated information between brain regions deserve further investigation. Indeed, dreaming during anaesthesia has been reported to occur in up to 27% of cases [105], and behaviourally unresponsive participants have been shown to perform mental imagery tasks during anaesthesia, both of which constitute cases of disconnected consciousness [106]. Thus, although our doses of propofol were consistent with the presence of SWAS, we cannot exclude that some of our participants may have been merely disconnected but still conscious, possibly driving the increases we observed.

More broadly, future research may also benefit from characterising the role of the synergistic workspace in the states of altered consciousness induced e.g. by psychedelics [107–109], especially since prominent involvement of the DMN has already been identified [110,111]. Likewise, the use of paradigms different from resting-state, such as measuring the brain's spontaneous responses to engaging stimuli (e.g. suspenseful narratives [112] or engaging movies [113]) may provide evidence for a more comprehensive understanding of brain changes during unconsciousness. Likewise, it will be of great interest to investigate whether and how reorganization of the synergistic global workspace is reflected in other indicators of consciousness [114], such as the brain's response to external perturbations – such as the EEG response to brief magnetic pulses used to compute the Perturbational Complexity Index, one of the most discriminative indices of consciousness available to date [115–119].

Additionally, the reliance here on 'resting-state' data without external stimuli may have resulted in an overestimation of the DMN's role in consciousness, and an under-estimation of the FPN (including lateral PFC), given their known different recruitment during no-task conditions [59]. Indeed, recent efforts have been carried out to obtain a data-driven characterisation of the brain's global workspace based on regions' involvement across multiple different tasks [5]. This work is complementary to ours in two aspects: first, the focus of Deco *et al.* [5] is on the role of the workspace related to cognition, whereas here we focus

primarily on consciousness. Second, by using transfer entropy as a measure of functional connectivity, Deco and colleagues [5] assessed the directionality of information exchange – whereas our measure of integrated information is undirected, but are able to distinguish between different kinds of information being exchanged and integrated. Thus, different ways of defining and characterising a global workspace in the human brain are possible, and can provide complementary insights about distinct aspects of the human neurocognitive architecture.

Looking forward, growing evidence indicates an important role for brain dynamics and time-resolved brain states in supporting cognition [7,18,120–127] and consciousness [41,93,128–135].Therefore, time-resolved extensions of our framework may shed further light on the dynamics of the synergistic workspace, especially if combined with neuroimaging modalities offering higher temporal resolution, such as magneto- or electroencephalography. More broadly, a key strength of our proposed cognitive architecture is its generality: being entirely grounded in the combination of information theory and network science, it could be applied to shed light on cognition in humans and other organisms [136], but also to inspire further development of artificial cognitive systems [137–141].

Conclusion

Overall, we have shown that powerful insights about human consciousness and neurocognitive architecture can be obtained through the information-resolved approach, afforded by the framework of Integrated Information Decomposition. Importantly, the proposed criteria to identify gateways, broadcasters, and the synergistic workspace itself, are based on practical network and information-theoretic tools, which are applicable to a broad range of neuroimaging datasets and neuroscientific questions. These findings bring us closer to a unified theoretical understanding of consciousness and its neuronal underpinnings - how mind arises from matter.

Materials and Methods

The propofol and DOC patient functional data employed in this study have been published before [41,107,142–146]. For clarity and consistency of reporting, where applicable we use the same wording as our previous work [41,107,142].

Briefly, the propofol anaesthesia data include anatomical and resting-state fMRI scans from n=16 subjects, scanned at rest before (“Awake”), during (“Anaesthesia”) and after (“Recovery”) propofol-induced loss of behavioural responsiveness. Data were acquired for 5 minutes with a TR of 2s. The DOC data include n=22 patients diagnosed with Unresponsive Wakefulness Syndrome/Vegetative State (N = 10) or Minimally Conscious State (N = 12) due to brain injury (Table S1). For each patient, in addition to anatomical scans, 256 functional volumes of resting-state fMRI were acquired, with a TR of 2s. Full details of recruitment and scanning are provided in the Supplementary Information.

Functional MRI preprocessing and denoising

The functional imaging data were preprocessed using a standard pipeline, implemented within the SPM12-based (http://www.fil.ion.ucl.ac.uk/spm) toolbox CONN (http://www.nitrc.org/projects/conn), version 17f [147]. The pipeline comprised the following steps: removal of the first five scans, to allow magnetisation to reach steady state; functional realignment and motion correction; slice-timing correction to account for differences in time of acquisition between slices; identification of outlier scans for subsequent regression by means of the quality assurance/artifact rejection software *art*

(http://www.nitrc.org/projects/artifact_detect); structure-function coregistration using each volunteer's high-resolution T1-weighted image; spatial normalisation to Montreal Neurological Institute (MNI-152) standard space with 2mm isotropic resampling resolution, using the segmented grey matter image , together with an *a priori* grey matter template.

To reduce noise due to cardiac, breathing, and motion artifacts, which are known to impact functional connectivity and network analyses [148,149], we applied the anatomical CompCor method of denoising the functional data [150], also implemented within the CONN toolbox. As for preprocessing, we followed the same denoising described in previous work [41,107,142]. The anatomical CompCor method involves regressing out of the functional data the following confounding effects: the first five principal components attributable to each individual's white matter signal, and the first five components attributable to individual cerebrospinal fluid (CSF) signal; six subject-specific realignment parameters (three translations and three rotations) as well as their first- order temporal derivatives; the artefacts identified by *art;* and main effect of scanning condition [150]. Linear detrending was also applied, and the subject-specific denoised BOLD signal timeseries were band-pass filtered to eliminate both low-frequency drift effects and high-frequency noise, thus retaining temporal frequencies between 0.008 and 0.09 Hz.

The step of global signal regression (GSR) has received substantial attention in the fMRI literature, as a potential denoising step [151–154]. However, GSR mathematically mandates that approximately 50% of correlations between regions will be negative [154], thereby removing potentially meaningful differences in the proportion of anticorrelations; additionally, it has been shown across species and states of consciousness that the global signal contains information relevant for consciousness [155]. Therefore, here we chose to avoid GSR in favour of the aCompCor denoising procedure, in line with previous work [41,107,142].

Due to the presence of deformations caused by brain injury, rather than relying on automated pipelines, DOC patients' brains were individually preprocessed using SPM12, with visual inspections after each step. Additionally, to further reduce potential movement artefacts, data underwent despiking with a hyperbolic tangent squashing function, also implemented from the CONN toolbox [147]. The remaining preprocessing and denoising steps were the same as described above.

Brain Parcellation

Brains were parcellated into 454 cortical and subcortical regions of interest (ROIs). The 400 cortical ROIs were obtained from the scale-400 version of the recent Schaefer local-global functional parcellation [50]. Since this parcellation only includes cortical regions, it was augmented with 54 subcortical ROIs from the highest resolution of the recent Tian parcellation [52]. We refer to this 454-ROI parcellation as the "augmented Schaefer" [49]. To ensure the robustness of our results to the choice of atlas, we also replicated them using an alternative cortical parcellation of different dimensionality: we used the Schaefer scale-200 cortical parcellation, complemented with the scale-32 subcortical ROIs from the Tian subcortical atlas [49]. The timecourses of denoised BOLD signals were averaged between all voxels belonging to a given atlas-derived ROI, using the CONN toolbox. The resulting region-specific timecourses of each subject were then extracted for further analysis in MATLAB.

HRF deconvolution

In accordance with our previous work [39,40] and previous studies using of information-theoretic measures in the context of functional MRI data, we used a dedicated toolbox [97] to deconvolve the hemodynamic response function from our regional BOLD signal timeseries prior to analysis.

Measuring Integrated Information

The framework of integrated information decomposition (ΦID) unifies integrated information theory (IIT) and partial information decomposition (PID) to decompose information flow into interpretable, disjoint parts. In this section we provide a brief description of ΦID and formulae required to compute the results in Figures 2 and 3. For further details, see [38,39].

Partial information decomposition

We begin with Shannon's Mutual information (MI), which quantifies the interdependence between two random variables *X* and *Y*. It is calculated as

$$I(X;Y) = H(X) - H(X|Y) = H(X) + H(Y) - H(X,Y) \tag{1}$$

where H(*X*) stands for the Shannon entropy of a variable *X*. Above, the first equality states that the mutual information is equal to the reduction in entropy (i.e., uncertainty) about *X* after *Y* is known. Put simply, the mutual information quantifies the information that one variable provides about another [156].

Crucially, Williams and Beer [33] observed that the information that two source variables *X* and *Y* give about a third target variable *Z*, I(*X,Y* ; *Z*), should be decomposable in terms of different *types* of information: information provided by one source but not the other (unique information), by both sources separately (redundant information), or jointly by their combination (synergistic information). Following this intuition, they developed the *Partial Information Decomposition* (PID; [33]) framework, which leads to the following fundamental decomposition:

$$\mathrm{I}(X,Y;Z) = \mathrm{Red}(X,Y;Z) + \mathrm{Un}(X;Z|Y) + \mathrm{Un}(Y;Z|X) + \mathrm{Syn}(X,Y;Z). \tag{2}$$

Above, *Un* corresponds to the unique information one source but the other doesn't, *Red* is the redundancy between both sources, and *Syn* is their synergy: information that neither *X* nor *Y* alone can provide, but that can be obtained by considering *X* and *Y* together.

The simplest example of a purely synergistic system is one in which *X* and *Y* are independent fair coins, and *Z* is determined by the exclusive-OR function *Z* = XOR(*X,Y*): i.e, *Z*=0 whenever *X* and *Y* have the same value, and *Z*=1 otherwise. It can be shown that *X* and *Y* are both statistically independent of *Z*, which implies that neither of them provide - by themselves - information about *Z*. However, *X* and *Y* together fully determine *Z*, hence the relationship between *Z* with *X* and *Y* is purely synergistic.

Recently, Mediano *et al* (2021) [38] formulated an extension of PID able to decompose the information that multiple source variables have about multiple target variables. This makes PID applicable to the dynamical systems setting, and yields a decomposition with redundant, unique, and synergistic components in the past and future that can be used as a principled method to analyse information flow in neural activity.

Synergy and redundancy calculation

While there is ongoing research on the advantages of different information decompositions for discrete data, most decompositions converge into the same simple form for the case of continuous Gaussian variables [157]. Known as *minimum mutual information PID* (MMI-PID), this decomposition quantifies redundancy in terms of the minimum mutual information of each individual source with the target; synergy, then, becomes identified with the additional information provided by the weaker source once the stronger source is known. Since linear-Gaussian models are sufficiently good descriptors of functional MRI timeseries (and more

complex, non-linear models offer no advantage [158,159]), here we adopt the MMI-PID decomposition, following our own and others' previous applications of PID to neuroscientific data [39].

In a dynamical system such as the brain, one can calculate the amount of information flowing from the system's past to its future, known as time-delayed mutual information (TDMI). Specifically, by denoting the past of variables as $X_{t-\tau}$ and $Y_{t-\tau}$ and treating them as sources, and their joint future state (X_t, Y_t), as target, one can apply the PID framework and decompose the information flowing from past to future as

$$\begin{aligned} I(X_{t-\tau}, Y_{t-\tau};\ X_t, Y_t\ ) \\ = Red(X_{t-\tau}, Y_{t-\tau};\ X_t, Y_t\ ) + Un(X_{t-\tau}; X_t, Y_t | Y_{t-\tau}) + Un(Y_{t-\tau}; X_t, Y_t | X_{t-\tau}) \\ + Syn(X_{t-\tau}, Y_{t-\tau};\ X_t, Y_t\ ) \end{aligned} \tag{3}$$

Applying ΦID to this quantity allows us to distinguish between redundant, unique, and synergistic information shared with respect to the future variables X_t, Y_t [38,39]. Importantly, this framework, has identified $Syn(X_{t-\tau}, Y_{t-\tau};\ X_t, Y_t\ )$ with the capacity of the system to exhibit emergent behaviour [160] as well as a stronger notion of redundancy, in which information is shared by X and Y in both past and future. Accordingly, using the MMI-ΦID decomposition for Gaussian variables, we use

$$Red(X, Y) = min\{\ I(X_{t-\tau};\ X_t), I(X_{t-\tau};\ Y_t), I(Y_{t-\tau};\ X_t), I(Y_{t-\tau};\ Y_t)\} \tag{4}$$

$$Syn(X, Y) = I(X_{t-\tau}, Y_{t-\tau};\ X_t, Y_t\ ) - max\{\ I(X_{t-\tau};\ X_t, Y_t\ ), I(Y_{t-\tau};\ X_t, Y_t\ )\}. \tag{5}$$

Here, we used the Gaussian solver implemented in the JIDT toolbox [161] to obtain TDMI, synergy and redundancy between each pair of brain regions, based on their HRF-deconvolved BOLD signal timeseries" [38,39].

Revised measure of integrated information from Integrated Information Decomposition

Through the framework of Integrated Information Decomposition, we can decompose the constituent elements of Φ, the formal measure of integrated information proposed by Integrated Information Theory to quantify consciousness [31]. Note that several variants of Φ have been proposed over the years, including the original formulation of Tononi [29], other formulations based on causal perturbation [99,100] and others (see [162,163] for comparative reviews). Here, we focus on the "empirical Φ" measure of Seth and Barrett [164], based on the measures by Balduzzi and Tononi (2008) [31] and adapted to applications to experimental data. It is computed as

$$\Phi = I(X_{t-\tau}, Y_{t-\tau};\ X_t, Y_t) - I(X_{t-\tau};\ X_t) - I(Y_{t-\tau};\ Y_t) \tag{6}$$

and it quantifies how much temporal information is contained in the system over and above the information in its past. This measure is easy to compute (compared with other Φ measures) [165] and represents a noteworthy attempt to formalise the powerful intuitions underlying IIT. However, once the original formulation from Balduzzi and Tononi is rendered suitable for practical empirical application [164,166] the resulting mathematical formulation has known shortcomings, including the fact that it can yield negative values in some cases - which are hard to interpret and seemingly paradoxical, as it does not seem plausible for a system to be "negatively integrated" or an organism to have negative consciousness [164,166].

Interestingly, with ΦID it can be formally demonstrated [38] that Φ is composed of different information atoms: it contains all the synergistic information in the system, the unique information transferred from X to Y and vice versa, and, importantly, the subtraction of redundancy (SI Figure 2A,B) - which explains why Φ can be negative in redundancy-dominated systems.

To address this fundamental shortcoming, Mediano, Rosas and colleagues [38] introduced a revised measure of integrated information, Φ_R, which consists of the original Φ with the redundancy added back in (SI Figure 2B),

$$\Phi_R = \Phi + Red(X, Y) \tag{7}$$

where Red(*X, Y*) is defined in Eq. (4). This measure is computationally tractable and preserves the original intuition of integrated information as measuring the extent to which "the whole is greater than the sum of its parts", since it captures only synergistic and transferred information. Crucially, thanks to Integrated Information Decomposition, it can be proved that the improved formulation of integrated information that we adopt here is guaranteed to be non-negative [38] - thereby avoiding a major conceptual limitation of the original formulation of Φ.

Note that the formula for Φ^{WMS} above stems from what is known as IIT 2.0, but TDMI is by no means the only way of quantifying the dynamical structure of a system: indeed, subsequent developments in IIT 3.0 used alternative metrics with a more explicit focus on causal interpretations [99], which were in turn replaced in the latest iteration known as IIT 4.0 [100,167]. We do not consider the alternative measure of integrated information proposed in IIT 3.0 because it is computationally intractable for systems bigger than a small set of logic gates, and it is not universally well-defined [166].

Gradient of redundancy-to-synergy relative importance to identify the synergistic workspace

After building networks of synergistic and redundant interactions between each pair of regions of interest (ROIs), we determined the role of each ROI in terms of its relative engagement in synergistic or redundant interactions. Following the procedure previously described [39], we first calculated the nodal strength of each brain region as the sum of all its connections in the group-averaged matrix. Then, we ranked all 454 regions based on their nodal strength (with higher-strength regions having higher ranks). This procedure was done separately for networks of synergy and redundancy. Subtracting each region's redundancy rank from its synergy rank yielded a gradient from negative (i.e., ranking higher in terms of redundancy than synergy) to positive (i.e., having a synergy rank higher than the corresponding redundancy rank; note that the sign is arbitrary).

It is important to note that the gradient is based on relative - rather than absolute - differences between regional synergy and redundancy; consequently, a positive rank difference does not necessarily mean that the region's synergy is greater than its redundancy; rather, it indicates that the balance between its synergy and redundancy relative to the rest of the brain is in favour of synergy - and *vice versa* for a negative gradient.

Subdivision of workspace nodes into gateways and broadcasters

To identify which regions within the workspace play the role of gateways or broadcasters postulated in our proposed architecture, we followed a procedure analogous to the one adopted to identify the gradient of redundancy-synergy relative importance, but replacing the node *strength* with the node *participation coefficient*. The participation coefficient P_i

quantifies the degree of connection that a node entertains with nodes belonging to other modules: the more of a node's connections are towards other modules, the higher its participation coefficient will be [48,168]. Conversely, the participation coefficient of a node will be zero if its connections are all with nodes belonging to its own module.

$$P_i = 1 - \sum_{s=1}^{M} \left(\frac{\kappa_{is}}{k_i}\right)^2 \tag{8}$$

Here, κ_{is} is the strength of positive connections between node *i* and other nodes in module *s*, k_i is the strength of all its positive connections, and *M* is the number of modules in the network. The participation coefficient ranges between zero (no connections with other modules) and one (equal connections to all other modules) [48,168].

Here, modules were set to be the seven canonical resting-state networks identified by Yeo and colleagues [51], into which the Schaefer parcellation is already divided [50], with the addition of an eighth subcortical network comprising all ROIs of the Tian subcortical network [52]. The brain's RSNs were chosen as modules because of their distinct and well-established functional roles, which fit well with the notion of modules as segregated and specialised processing systems interfacing with the global workspace. Additionally, having the same definition of modules (i.e., RSNs) for synergy and redundancy allowed us to compute their respective participation coefficients in an unbiased way.

Separately for connectivity matrices of synergy and redundancy, the participation coefficient of each brain region was calculated. Then, regions belonging to the synergistic workspace were ranked, so that higher ranks indicated higher participation coefficient. Finally, the redundancy-based participation coefficient rank of each workspace region was subtracted from its corresponding synergy-based participation coefficient rank, to quantify – within the workspace – whether regions have relatively more diverse connectivity in terms of synergy, or in terms of redundancy.

This procedure yielded a gradient over workspace regions, from negative (i.e. having a more highly ranked participation coefficient based on redundancy than synergy) to positive (i.e. having a more highly ranked participation coefficient based on synergy than redundancy). Note that as before, the sign of this gradient is arbitrary, and it is based on relative rather than absolute difference. Workspace regions with a positive gradient value were classified as "gateways", since they have synergistic connections with many brain modules. In contrast, workspace regions with a negative value of the gradient - i.e. those whose redundancy rank is higher than their synergy rank, in terms of participation coefficient - were labelled as workspace "broadcasters", since they possess information that is duplicated across multiple modules in the brain.

Statistical Analysis

Network Based Statistic

The network-based statistic approach [54] was used to investigate the statistical significance of propofol-induced or DOC-induced alterations. This nonparametric statistical method is designed to control the family-wise error due to multiple comparisons, for application to graph data. Connected components of the graph are identified from edges that survive an a-priori statistical threshold (F-contrast; here we set the threshold to an F-value of 9, two-sided, with an alpha level of 0.05). In turn, the statistical significance of such connected components is estimated by comparing their topology against a null distribution of the size of connected components obtained from non-parametric permutation testing. This approach

rejects the null hypothesis on a component-by-component level, and therefore achieves superior power compared to mass-univariate approaches [54].

Testing for shared effects across datasets

We sought to detect changes that are common across datasets, to rule out possible propofol- or DOC-specific effects that are not related to consciousness per se [41]. To this end, we employed a null hypothesis significance test under the composite null hypothesis that *at least* one dataset among those considered here has no effect. In other words, for the null hypothesis to be rejected we demand that all comparisons exhibit non-zero effects. As usual, the test proceeds by comparing an observed test statistic with a null distribution. The test statistic is the minimum of the three F-scores obtained in the comparisons of interest (DOC vs awake; anaesthesia vs awake; and anaesthesia vs recovery), and the null distribution is sampled by randomly reshuffling exactly one dataset (picked at random) at a time and recalculating the F-scores. By shuffling exactly one dataset (instead of all of them), we are comparing the observed data against the "least altered" version of the data that is still compatible with the null hypothesis. This is a type of least favourable configuration test [169], which is guaranteed to control the false positive rate below a set threshold (here, 0.05). The details of this test will be described in a future publication. Common changes across the three states of consciousness were then identified as edges (defined in terms of Φ_R) that were either (i) increased in DOC compared with control; (ii) increased during anaesthesia compared with wakefulness; and (iii) increased during anaesthesia compared with post-anaesthetic recovery; or (i) decreased in DOC compared with control; (ii) decreased during anaesthesia compared with wakefulness; and (iii) decreased during anaesthesia compared with post-anaesthetic recovery.

Acknowledgments

Author AIL is grateful to Dr. Athena Demertzi and Dr. Petra Vertes for helpful discussion. This work was supported by grants from the UK Medical Research Council [U.1055.01.002.00001.01 to AMO and JDP]; The James S. McDonnell Foundation [to AMO and JDP]; and the Canada Excellence Research Chairs program (215063 to AMO); the National Institute for Health Research (NIHR, UK), Cambridge Biomedical Research Centre and NIHR Senior Investigator Awards [to DKM], the Stephen Erskine Fellowship (Queens' College, Cambridge, to EAS), the L'Oreal-Unesco for Women in Science Excellence Research Fellowship to LN; the British Oxygen Professorship of the Royal College of Anaesthetists [to DKM] and the Gates Cambridge Trust (to AIL). PAM and DB are funded by the Wellcome Trust (grant no. 210920/Z/18/Z). FR is funded by the Ad Astra Chandaria foundation. The research was also supported by the NIHR Brain Injury Healthcare Technology Co-operative based at Cambridge University Hospitals NHS Foundation Trust and University of Cambridge. AMO and DKM are Fellows of the CIFAR Brain, Mind, and Consciousness Programme. Data were provided [in part] by the Human Connectome Project, WU-Minn Consortium (Principal Investigators: David Van Essen and Kamil Ugurbil; 1U54MH091657) funded by the 16 NIH Institutes and Centers that support the NIH Blueprint for Neuroscience Research; and by the McDonnell Center for Systems Neuroscience at Washington University.

Author Contributions: AIL: conceived the study; analysed data; wrote first draft of the manuscript. PAM: conceived the study; contributed to data analysis and interpretation of results; reviewed and edited the manuscript. FR: contributed to data analysis and interpretation of results; reviewed and edited the manuscript. M.M.C.: contributed to data analysis. DKM: reviewed the manuscript. RCH: reviewed the manuscript and contributed to interpretation of results. DB: conceived the study; reviewed and edited the manuscript. EAS: conceived the study; reviewed and edited the manuscript. P.F., G.B.W., J.A., J.D.P., A.M.O.,

L.N., D.K.M. and E.A.S. were involved in designing the original studies for which the present data were collected. P.F., M.M.C., G.B.W., J.A., L.N. and E.A.S. all participated in data collection.

Competing Interest Statement: The authors declare no competing interests.

References

1. Varela, F., Lachaux, J.P., Rodriguez, E., and Martinerie, J. (2001). The brainweb: Phase synchronization and large-scale integration. Nature Reviews Neuroscience *2*, 229–239. 10.1038/35067550.

2. Petersen, S.E., and Sporns, O. (2015). Brain Networks and Cognitive Architectures. Neuron *88*, 207–219. 10.1016/j.neuron.2015.09.027.

3. Shine, J.M. (2019). Neuromodulatory Influences on Integration and Segregation in the Brain. Trends in Cognitive Sciences *23*, 572–583. 10.1016/j.tics.2019.04.002.

4. Fodor, J.A. (1985). Précis of *The Modularity of Mind*. Behavioral and Brain Sciences *8*, 1–5. 10.1017/S0140525X0001921X.

5. Deco, G., Vidaurre, D., and Kringelbach, M.L. (2021). Revisiting the global workspace: Orchestration of the functional hierarchical organisation of the human brain. Nature Human Behaviour *5*. 10.1101/859579.

6. Assem, M., Glasser, M.F., Van Essen, D.C., and Duncan, J. (2020). A Domain-General Cognitive Core Defined in Multimodally Parcellated Human Cortex. Cerebral Cortex *30*, 4361–4380. 10.1093/cercor/bhaa023.

7. Shine, J.M., Breakspear, M., Bell, P.T., Ehgoetz Martens, K., Shine, R., Koyejo, O., Sporns, O., and Poldrack, R.A. (2019). Human cognition involves the dynamic integration of neural activity and neuromodulatory systems. Nature Neuroscience *22*, 289–296. 10.1038/s41593-018-0312-0.

8. Hagmann, P., Cammoun, L., Gigandet, X., Meuli, R., and Honey, C.J. (2008). Mapping the structural core of human cerebral cortex. PLoS Biol *6*, 159. 10.1371/journal.pbio.0060159.

9. Felleman, D.J., and Van Essen, D.C. (1991). Distributed hierarchical processing in the primate cerebral cortex. Cerebral Cortex *1*, 1–47. 10.1093/cercor/1.1.1.

10. Goulas, A., Changeux, J.P., Wagstyl, K., Amunts, K., Palomero-Gallagher, N., and Hilgetag, C.C. (2021). The natural axis of transmitter receptor distribution in the human cerebral cortex. Proceedings of the National Academy of Sciences of the United States of America *118*. 10.1073/PNAS.2020574118.

11. Sydnor, V.J., Larsen, B., Bassett, D.S., Alexander-Bloch, A., Fair, D.A., Liston, C., Mackey, A.P., Milham, M.P., Pines, A., Roalf, D.R., et al. (2021). Neurodevelopment of the association cortices: Patterns, mechanisms, and implications for psychopathology. Neuron *109*, 2820–2846. 10.1016/j.neuron.2021.06.016.

12. Baum, G.L., Cui, Z., Roalf, D.R., Ciric, R., Betzel, R.F., Larsen, B., Cieslak, M., Cook, P.A., Xia, C.H., Moore, T.M., et al. (2020). Development of structure–function coupling in human brain networks during youth. Proceedings of the National Academy of Sciences of the United States of America *117*, 771–778. 10.1073/pnas.1912034117.

13. Bertolero, M.A., Yeo, B.T.T., and D'Esposito, M. (2017). The diverse club. Nature Communications *8*, 1277. 10.1038/s41467-017-01189-w.

14. Vázquez-Rodríguez, B., Suárez, L.E., Markello, R.D., Shafiei, G., Paquola, C., Hagmann, P., Van Den Heuvel, M.P., Bernhardt, B.C., Spreng, R.N., and Misic, B. (2019). Gradients of structure–function tethering across neocortex. Proceedings of the National Academy of Sciences of the United States of America *116*, 21219–21227. 10.1073/pnas.1903403116.

15. Margulies, D.S., Ghosh, S.S., Goulas, A., Falkiewicz, M., Huntenburg, J.M., Langs, G., Bezgin, G., Eickhoff, S.B., Castellanos, F.X., Petrides, M., et al. (2016). Situating the default-mode network along a principal gradient of macroscale cortical organization. Proceedings of the National Academy of Sciences of the United States of America *113*, 12574–12579. 10.1073/pnas.1608282113.

16. Burt, J.B., Demirtaş, M., Eckner, W.J., Navejar, N.M., Ji, J.L., Martin, W.J., Bernacchia, A., Anticevic, A., and Murray, J.D. (2018). Hierarchy of transcriptomic specialization across human cortex captured by structural neuroimaging topography. Nature Neuroscience *21*, 1251–1259. 10.1038/s41593-018-0195-0.

17. Demirtaş, M., Burt, J.B., Helmer, M., Ji, J.L., Adkinson, B.D., Glasser, M.F., Van Essen, D.C., Sotiropoulos, S.N., Anticevic, A., and Murray, J.D. (2019). Hierarchical Heterogeneity across Human Cortex Shapes Large-Scale Neural Dynamics. Neuron *101*, 1181-1194.e13. 10.1016/j.neuron.2019.01.017.

18. Deco, G., Kringelbach, M.L., Arnatkeviciute, A., Oldham, S., Sabaroedin, K., Rogasch, N.C., Aquino, K.M., and Fornito, A. (2021). Dynamical consequences of regional heterogeneity in the brain's transcriptional landscape. Science Advances *7*, eabf4752. 10.1126/SCIADV.ABF4752.

19. Hansen, J.Y., Markello, R.D., Vogel, J.W., Seidlitz, J., Bzdok, D., and Misic, B. (2021). Mapping gene transcription and neurocognition across human neocortex. Nature Human Behaviour *5*, 1240–1250. 10.1038/s41562-021-01082-z.

20. Hansen, J.Y., Shafiei, G., Markello, R.D., Smart, K., Cox, S., Norgaard, M., Beliveau, V., Wu, Y., Gallezot, J.-D., Aumont, E., et al. (2022). Mapping neurotransmitter systems to the structural and functional organization of the human neocortex. Nature Neuroscience *25*, 1569–1581.

21. Tononi, G., Boly, M., Massimini, M., and Koch, C. (2016). Integrated information theory: From consciousness to its physical substrate. Nature Reviews Neuroscience *17*, 450–461. 10.1038/nrn.2016.44.

22. Seth, A.K., and Bayne, T. (2022). Theories of consciousness. Nature reviews. Neuroscience. 10.1038/S41583-022-00587-4.

23. Dehaene, S., and Changeux, J.-P. (2011). Experimental and Theoretical Approaches to Conscious Processing. Neuron *70*, 200–227. 10.1016/j.neuron.2011.03.018.

24. Mashour, G.A., Roelfsema, P., Changeux, J.P., and Dehaene, S. (2020). Conscious Processing and the Global Neuronal Workspace Hypothesis. Neuron *105*, 776–798. 10.1016/j.neuron.2020.01.026.

25. Dehaene, S., Changeux, J.P., and Naccache, L. (2011). The global neuronal workspace model of conscious access: From neuronal architectures to clinical applications. Research and Perspectives in Neurosciences *18*, 55–84. 10.1007/978-3-642-18015-6_4.

26. Baars, B.J. (2005). Global workspace theory of consciousness: Toward a cognitive neuroscience of human experience. Progress in Brain Research *150*, 45–53. 10.1016/S0079-6123(05)50004-9.

27. Dehaene, S., and Naccache, L. (2001). Towards a cognitive neuroscience of consciousness: Basic evidence and a workspace framework. Cognition *79*, 1–37. 10.1016/S0010-0277(00)00123-2.

28. Tononi, G. (2008). Consciousness as Integrated Information. The Biological Bulletin *215*, 216–242. 215/3/216 [pii].

29. Tononi, G. (2004). An information integration theory of consciousness. BMC Neuroscience *5*, 42–64. 10.1186/1471-2202-5-42.

30. Tononi, G., Edelman, G.M., and Sporns, O. (1998). Complexity and coherency: Integrating information in the brain. Trends in Cognitive Sciences *2*, 474–484. 10.1016/S1364-6613(98)01259-5.

31. Balduzzi, D., and Tononi, G. (2008). Integrated information in discrete dynamical systems: Motivation and theoretical framework. PLoS Computational Biology *4*. 10.1371/journal.pcbi.1000091.

32. Cavanna, F., Vilas, M.G., Palmucci, M., and Tagliazucchi, E. (2018). Dynamic functional connectivity and brain metastability during altered states of consciousness. NeuroImage *180*, 383–395. 10.1016/j.neuroimage.2017.09.065.

33. Williams, P.L., and Beer, R.D. (2010). Nonnegative Decomposition of Multivariate Information. arXiv, http://arxiv.org/abs/1004.2515.

34. Varley, T.F., Sporns, O., Schaffelhofer, S., Scherberger, H., and Dann, B. (2023). Information-processing dynamics in neural networks of macaque cerebral cortex reflect cognitive state and behavior. Proc Natl Acad Sci U S A *120*, e2207677120. 10.1073/pnas.2207677120.

35. Timme, N., Alford, W., Flecker, B., and Beggs, J.M. (2014). Synergy, redundancy, and multivariate information measures: An experimentalist's perspective. Journal of Computational Neuroscience *36*, 119–140. 10.1007/s10827-013-0458-4.

36. Sherrill, S.P., Timme, N., Beggs, J., and Newman, E.L. (2021). Partial information decomposition reveals that synergistic neural integration is greater downstream of recurrent information flow in organotypic cortical cultures. 1–28. 10.1371/journal.pcbi.1009196.

37. Faber, S.P., Timme, N.M., Beggs, J.M., and Newman, E.L. (2019). Computation is concentrated in rich clubs of local cortical networks. Network Neuroscience *3*, 384–404. 10.1162/netn_a_00069.

38. Mediano, P.A.M., Rosas, F.E., Luppi, A.I., Carhart-Harris, R.L., Bor, D., Seth, A.K., and Barrett, A.B. (2021). Towards an extended taxonomy of information dynamics via Integrated Information Decomposition. arXiv.

39. Luppi, A.I., Mediano, P.A.M., Rosas, F.E., Holland, N., Fryer, T.D., O'Brien, J.T., Rowe, J.B., Menon, D.K., Bor, D., and Stamatakis, E.A. (2022). A synergistic core for human brain evolution and cognition. Nat Neurosci *25*, 771–782. 10.1038/s41593-022-01070-0.

40. Luppi, A.I., Mediano, P.A.M., Rosas, F.E., Allanson, J., Pickard, J.D., Williams, G.B., Craig, M.M., Finoia, P., Peattie, A.R.D., Coppola, P., et al. (2023). Reduced emergent character of neural dynamics in patients with a disrupted connectome. Neuroimage, 119926. 10.1016/j.neuroimage.2023.119926.

41. Luppi, A.I., Craig, M.M., Pappas, I., Finoia, P., Williams, G.B., Allanson, J., Pickard, J.D., Owen, A.M., Naci, L., Menon, D.K., et al. (2019). Consciousness-specific dynamic interactions of brain integration and functional diversity. Nature Communications *10*. 10.1038/s41467-019-12658-9.

42. Tsitsiklis, J.N. (1989). Decentralized Detection. In Advances in Statistical Signal Processing, Vol 2: Signal Detection.

43. Veeravalli, V.V., and Varshney, P.K. (2012). Distributed inference in wireless sensor networks. Trans. R. Soc. A *370*, 100–117. 10.1098/rsta.2011.0194.

44. Lever, K.E., Merabti, M., and Kifayat, K. (2013). Single Points of Failure Within Systems-of-Systems. 14th Annual Post Graduate Symposium on the Convergence of Telecommunications, Networking and Broadcasting (PGNet), 183–188.

45. Rosas, F., Hsiao, J.H., and Chen, K.C. (2017). A technological perspective on information cascades via social learning. IEEE Access *5*, 22605–22633. 10.1109/ACCESS.2017.2687422.

46. Sneve, M.H., Grydeland, H., Rosa, M.G.P., Paus, T., Chaplin, T., Walhovd, K., and Fjell, A.M. (2019). High-expanding regions in primate cortical brain evolution support supramodal cognitive flexibility. Cerebral Cortex *29*, 3891–3901. 10.1093/cercor/bhy268.

47. Shanahan, M. (2012). The brain's connective core and its role in animal cognition. Philosophical Transactions of the Royal Society B: Biological Sciences *367*, 2704–2714. 10.1098/rstb.2012.0128.

48. Rubinov, M., and Sporns, O. (2010). Complex network measures of brain connectivity: Uses and interpretations. NeuroImage *52*, 1059–1069. 10.1016/j.neuroimage.2009.10.003.

49. Luppi, A.I., and Stamatakis, E.A. (2021). Combining network topology and information theory to construct representative brain networks. Network Neuroscience *5*, 96–124. 10.1162/netn_a_00170.

50. Schaefer, A., Kong, R., Gordon, E.M., Laumann, T.O., Zuo, X.-N., Holmes, A.J., Eickhoff, S.B., and Yeo, B.T.T. (2018). Local-Global Parcellation of the Human Cerebral Cortex from Intrinsic Functional Connectivity MRI. Cerebral Cortex *28*, 3095–3114. 10.1093/cercor/bhx179.

51. Yeo, B.T.T., Krienen, F.M., Sepulcre, J., Sabuncu, M.R., Lashkari, D., Hollinshead, M., Roffman, J.L., Smoller, J.W., Zollei, L., Polimeni, J.R., et al. (2011). The organization of the human cerebral cortex estimated by intrinsic functional connectivity. Journal of neurophysiology *106*, 1125–1165. 10.1152/jn.00338.2011.

52. Tian, Y., Margulies, D.S., Breakspear, M., and Zalesky, A. (2020). Topographic organization of the human subcortex unveiled with functional connectivity gradients. Nature Neuroscience *23*, 1421–1432. 10.1038/s41593-020-00711-6.

53. Bor, D., and Seth, A.K. (2012). Consciousness and the prefrontal parietal network: Insights from attention, working memory, and chunking. Frontiers in Psychology *3*. 10.3389/fpsyg.2012.00063.

54. Zalesky, A., Fornito, A., and Bullmore, E.T. (2010). Network-based statistic: Identifying differences in brain networks. NeuroImage *53*, 1197–1207. 10.1016/j.neuroimage.2010.06.041.

55. Fedorenko, E., Duncan, J., and Kanwisher, N. (2013). Broad domain generality in focal regions of frontal and parietal cortex. Proceedings of the National Academy of Sciences of the United States of America *110*, 16616–16621. 10.1073/pnas.1315235110.

56. Duncan, J., and Owen, A.M. (2000). Common regions of the human frontal lobe recruited by diverse cognitive demands. Trends in Neurosciences *23*, 475–483. 10.1016/S0166-2236(00)01633-7.

57. Barbey, A.K. (2018). Network Neuroscience Theory of Human Intelligence. Trends in Cognitive Sciences *22*, 8–20. 10.1016/j.tics.2017.10.001.

58. Gu, S., Pasqualetti, F., Cieslak, M., Telesford, Q.K., Yu, A.B., Kahn, A.E., Medaglia, J.D., Vettel, J.M., Miller, M.B., Grafton, S.T., et al. (2015). Controllability of structural brain networks. Nature Communications *6*, 8414. 10.1038/ncomms9414.

59. Fox, M.D., Snyder, A.Z., Vincent, J.L., Corbetta, M., Van Essen, D.C., and Raichle, M.E. (2005). The human brain is intrinsically organized into dynamic, anticorrelated functional networks. Proceedings of the National Academy of Sciences *102*, 9673–9678. 10.1073/pnas.0504136102.

60. Raichle, M.E., MacLeod, A.M., Snyder, A.Z., Powers, W.J., Gusnard, D.A., and Shulman, G.L. (2001). A default mode of brain function. Proceedings of the National Academy of Sciences of the United States of America *98*, 676–682. 10.1073/pnas.98.2.676.

61. Raichle, M.E. (2015). The Brain's Default Mode Network. Annual Review of Neuroscience *38*, 433–447. 10.1146/annurev-neuro-071013-014030.

62. Wei, Y., de Lange, S.C., Scholtens, L.H., Watanabe, K., Ardesch, D.J., Jansen, P.R., Savage, J.E., Li, L., Preuss, T.M., Rilling, J.K., et al. (2019). Genetic mapping and evolutionary analysis of human-expanded cognitive networks. Nature Communications *10*. 10.1038/s41467-019-12764-8.

63. Xu, T., Nenning, K.H., Schwartz, E., Hong, S.J., Vogelstein, J.T., Goulas, A., Fair, D.A., Schroeder, C.E., Margulies, D.S., Smallwood, J., et al. (2020). Cross-species functional alignment reveals evolutionary hierarchy within the connectome. NeuroImage *223*. 10.1016/j.neuroimage.2020.117346.

64. Huntenburg, J.M., Bazin, P.-L., and Margulies, D.S. (2018). Large-Scale Gradients in Human Cortical Organization. Trends Cogn Sci *22*, 21–31. 10.1016/j.tics.2017.11.002.

65. Smallwood, J., Bernhardt, B.C., Leech, R., Bzdok, D., Jefferies, E., and Margulies, D.S. (2021). The default mode network in cognition: a topographical perspective. Nature Reviews Neuroscience *22*, 503–513. 10.1038/s41583-021-00474-4.

66. Deco, G., Kringelbach, M.L., Jirsa, V.K., and Ritter, P. (2017). The dynamics of resting fluctuations in the brain: Metastability and its dynamical cortical core. Scientific Reports *7*, 1–14. 10.1038/s41598-017-03073-5.

67. Kabbara, A., EL Falou, W., Khalil, M., Wendling, F., and Hassan, M. (2017). The dynamic functional core network of the human brain at rest. Scientific Reports *7*, 2936. 10.1038/s41598-017-03420-6.

68. de Pasquale, F., Della Penna, S., Snyder, A.Z., Marzetti, L., Pizzella, V., Romani, G.L., and Corbetta, M. (2012). A Cortical Core for Dynamic Integration of Functional Networks in the Resting Human Brain. Neuron *74*, 753–764. 10.1016/j.neuron.2012.03.031.

69. Vatansever, D., Menon, X.D.K., Manktelow, A.E., Sahakian, B.J., and Stamatakis, E.A. (2015). Default Mode Dynamics for Global Functional Integration. The Journal of neuroscience : the official journal of the Society for Neuroscience *35*, 15254–15262. 10.1523/JNEUROSCI.2135-15.2015.

70. Vatansever, D., Menon, D.K., and Stamatakis, E.A. (2017). Default mode contributions to automated information processing. Proceedings of the National Academy of Sciences of the United States of America *114*, 12821–12826. 10.1073/pnas.1710521114.

71. Chiou, R., Humphreys, G.F., and Lambon Ralph, M.A. (2020). Bipartite functional fractionation within the default network supports disparate forms of internally oriented cognition. Cerebral Cortex *30*, 5484–5501. 10.1093/cercor/bhaa130.

72. Cavanna, A.E., and Trimble, M.R. (2006). The precuneus: A review of its functional anatomy and behavioural correlates. Brain *129*, 564–583. 10.1093/brain/awl004.

73. Qin, P., and Northoff, G. (2011). How is our self related to midline regions and the default-mode network? NeuroImage *57*, 1221–1233. 10.1016/j.neuroimage.2011.05.028.

74. Karapanagiotidis, T., Bernhardt, B.C., Jefferies, E., and Smallwood, J. (2017). Tracking thoughts: Exploring the neural architecture of mental time travel during mind-wandering. NeuroImage *147*, 272–281. 10.1016/j.neuroimage.2016.12.031.

75. Buckner, R.L., Andrews-Hanna, J.R., and Schacter, D.L. (2008). The brain's default network: Anatomy, function, and relevance to disease. Annals of the New York Academy of Sciences *1124*, 1–38. 10.1196/annals.1440.011.

76. Buckner, R.L., and DiNicola, L.M. (2019). The brain's default network: updated anatomy, physiology and evolving insights. Nature Reviews Neuroscience *20*, 593–608. 10.1038/s41583-019-0212-7.

77. Schacter, D.L., Addis, D.R., and Buckner, R.L. (2007). Remembering the past to imagine the future: the prospective brain. Nature Reviews Neuroscience *8*, 657–661. 10.1080/08995600802554748.

78. Szpunar, K.K., Spreng, R.N., and Schacter, D.L. (2014). A taxonomy of prospection: Introducing an organizational framework for future-oriented cognition. Proceedings of the National Academy of Sciences of the United States of America *111*, 18414–18421. 10.1073/pnas.1417144111.

79. Hassabis, D., and Maguire, E.A. (2009). The construction system of the brain. Philosophical Transactions of the Royal Society B: Biological Sciences *364*, 1263–1271. 10.1098/rstb.2008.0296.

80. Wen, T., Mitchell, D.J., and Duncan, J. (2020). The Functional Convergence and Heterogeneity of Social, Episodic, and Self-Referential Thought in the Default Mode Network. Cerebral cortex *30*, 5915–5929. 10.1093/cercor/bhaa166.

81. Wang, X., Margulies, D.S., Smallwood, J., and Jefferies, E. (2020). A gradient from long-term memory to novel cognition: Transitions through default mode and executive cortex. NeuroImage *220*. 10.1016/j.neuroimage.2020.117074.

82. Dohmatob, E., Dumas, G., and Bzdok, D. (2020). Dark control: The default mode network as a reinforcement learning agent. Human Brain Mapping *41*, 3318–3341. 10.1002/hbm.25019.

83. Yeshurun, Y., Nguyen, M., and Hasson, U. (2021). The default mode network: where the idiosyncratic self meets the shared social world. Nature Reviews Neuroscience *22*, 181–192. 10.1038/s41583-020-00420-w.

84. Shanahan, M. (2010). Embodiment and the Inner Life: Cognition and Consciousness in the Space of Possible Minds (Oxford University Press) 10.1093/acprof:oso/9780199226559.001.0001.

85. MacDonald, A.A., Naci, L., MacDonald, P.A., and Owen, A.M. (2015). Anesthesia and neuroimaging: Investigating the neural correlates of unconsciousness. Trends in Cognitive Sciences *19*, 100–107. 10.1016/j.tics.2014.12.005.

86. Hannawi, Y., Lindquist, M.A., Caffo, B.S., Sair, H.I., and Stevens, R.D. (2015). Resting brain activity in disorders of consciousness: a systematic review and meta-analysis. Neurology *84*, 1272–1280. 10.1212/WNL.0000000000001404; 10.1212/WNL.0000000000001404.

87. Vanhaudenhuyse, A., Quentin Noirhomme, Ã., Luaba J-F Tshibanda, Ã., Bruno, M.-A., Boveroux, P., Schnakers, C., Soddu, A., Perlbarg, V., Ledoux, D., Brichant, J.-F., et al. (2010). Default network connectivity reflects the level of consciousness in non-communicative brain-damaged patients. Brain *133*, 161–171. 10.1093/brain/awp313.

88. Di Perri, C., Amico, E., Heine, L., Annen, J., Martial, C., Larroque, S.K., Soddu, A., Marinazzo, D., and Laureys, S. (2018). Multifaceted brain networks reconfiguration in disorders of consciousness uncovered by co-activation patterns. Human Brain Mapping *39*, 89–103. 10.1002/hbm.23826.

89. Demertzi, A., Antonopoulos, G., Heine, L., Voss, H.U., Crone, J.S., De Los Angeles, C., Bahri, M.A., Di Perri, C., Vanhaudenhuyse, A., Charland-Verville, V., et al. (2015). Intrinsic functional

connectivity differentiates minimally conscious from unresponsive patients. Brain *138*, 2619–2631. 10.1093/brain/awv169.

90. Boveroux, P., Vanhaudenhuyse, A., and Phillips, C. (2010). Breakdown of within- and between-network Resting State during Propofol-induced Loss of Consciousness. Anesthesiology *113*, 1038–1053.

91. Bodien, Y.G., Threlkeld, Z.D., and Edlow, B.L. (2019). Default mode network dynamics in covert consciousness. Cortex *119*, 571–574. 10.1016/j.cortex.2019.01.014.

92. Spindler, L.R.B., Luppi, A.I., Adapa, R.M., Craig, M.M., Coppola, P., Peattie, A.R.D., Manktelow, A.E., Finoia, P., Sahakian, B.J., Williams, G.B., et al. (2021). Dopaminergic brainstem disconnection is common to pharmacological and pathological consciousness perturbation. Proceedings of the National Academy of Sciences of the United States of America *118*, e2026289118. 10.1073/pnas.2026289118.

93. Huang, Z., Zhang, J., Wu, J., Mashour, G.A., and Hudetz, A.G. (2020). Temporal circuit of macroscale dynamic brain activity supports human consciousness. Science Advances *6*, 87–98. 10.1126/sciadv.aaz0087.

94. Fischer, D., Snider, S.B., Barra, M.E., Sanders, W.R., Rapalino, O., Schaefer, P., Foulkes, A.S., Bodien, Y.G., and Edlow, B.L. (2022). Disorders of Consciousness Associated With COVID-19. Neurology *98*, e315–e325. 10.1212/WNL.0000000000013067.

95. Ní Mhuircheartaigh, R., Warnaby, C., Rogers, R., Jbabdi, S., and Tracey, I. (2013). Slow-wave activity saturation and thalamocortical isolation during propofol anesthesia in humans. Science translational medicine *5*, 208ra148. 10.1126/scitranslmed.3006007.

96. Warnaby, C.E., Sleigh, J.W., Hight, D., Jbabdi, S., and Tracey, I. (2017). Investigation of Slow-wave Activity Saturation during Surgical Anesthesia Reveals a Signature of Neural Inertia in Humans. Anesthesiology *127*, 645–657. 10.1097/ALN.0000000000001759.

97. Wu, G.R., Liao, W., Stramaglia, S., Ding, J.R., Chen, H., and Marinazzo, D. (2013). A blind deconvolution approach to recover effective connectivity brain networks from resting state fMRI data. Medical Image Analysis *17*, 365–374. 10.1016/j.media.2013.01.003.

98. Wu, G.R., Di Perri, C., Charland-Verville, V., Martial, C., Carrière, M., Vanhaudenhuyse, A., Laureys, S., and Marinazzo, D. (2019). Modulation of the spontaneous hemodynamic response function across levels of consciousness. NeuroImage *200*, 450–459. 10.1016/j.neuroimage.2019.07.011.

99. Oizumi, M., Albantakis, L., and Tononi, G. (2014). From the Phenomenology to the Mechanisms of Consciousness: Integrated Information Theory 3.0. PLoS Computational Biology *10*. 10.1371/journal.pcbi.1003588.

100. Albantakis, L., Barbosa, L., Findlay, G., Grasso, M., Haun, A.M., Marshall, W., Mayner, W.G., Zaeemzadeh, A., Boly, M., Juel, B.E., et al. (2022). Integrated information theory (IIT) 4.0: Formulating the properties of phenomenal existence in physical terms. 10.48550/arXiv.2212.14787.

101. Hoel, E.P., Albantakis, L., and Tononi, G. (2013). Quantifying causal emergence shows that macro can beat micro. Proceedings of the National Academy of Sciences of the USA *110*, 19790–19795. 10.1073/pnas.1314922110.

102. Hoel, E.P., Albantakis, L., Marshall, W., and Tononi, G. (2016). Can the macro beat the micro? Integrated information across spatiotemporal scales. Neuroscience of Consciousness, 1–13. 10.1093/nc/niw012.

103. Klein, B., and Hoel, E. (2020). The Emergence of Informative Higher Scales in Complex Networks. Complexity *2020*. 10.1155/2020/8932526.

104. Varley, T., and Hoel, E. (2021). Emergence as the conversion of information: A unifying theory. arXiv.

105. Leslie, Kate., Skrzypek, Hannah., Paech, M.J., Kurowski, Irina., and Whybrow, Tracey. (2007). Dreaming During Anesthesia and Anesthetic Depth in Elective Surgery Patients. Anesthesiology *106*, 33–42. 10.1097/00000542-200701000-00010.

106. Huang, Z., Vlisides, P.E., Tarnal, V.C., Janke, E.L., Keefe, K.M., Collins, M.M., McKinney, A.M., Picton, P., Harris, R.E., Mashour, G.A., et al. (2018). Brain imaging reveals covert consciousness during behavioral unresponsiveness induced by propofol. Scientific Reports *8*, 1–11. 10.1038/s41598-018-31436-z.

107. Luppi, A.I., Vohryzek, J., Kringelbach, M.L., Mediano, P.A.M., Craig, M.M., Adapa, R., Carhart-Harris, R.L., Roseman, L., Pappas, I., Peattie, A.R.D., et al. (2023). Distributed harmonic patterns of structure-function dependence orchestrate human consciousness. Commun Biol *6*, 1–19. 10.1038/s42003-023-04474-1.

108. Huang, Z., Mashour, G.A., and Hudetz, A.G. (2023). Functional geometry of the cortex encodes dimensions of consciousness. Nat Commun *14*, 72. 10.1038/s41467-022-35764-7.

109. Timmermann, C., Roseman, L., Haridas, S., Rosas, F.E., Luan, L., Kettner, H., Martell, J., Erritzoe, D., Tagliazucchi, E., Pallavicini, C., et al. (2023). Human brain effects of DMT assessed via EEG-fMRI. Proceedings of the National Academy of Sciences *120*, e2218949120. 10.1073/pnas.2218949120.

110. Carhart-Harris, R.L. (2018). The entropic brain - revisited. Neuropharmacology *142*, 167–178. 10.1016/j.neuropharm.2018.03.010.

111. Carhart-Harris, R.L., Muthukumaraswamy, S., Roseman, L., Kaelen, M., Droog, W., Murphy, K., Tagliazucchi, E., Schenberg, E.E., Nest, T., Orban, C., et al. (2016). Neural correlates of the LSD experience revealed by multimodal neuroimaging. Proceedings of the National Academy of Sciences *113*, 201518377. 10.1073/pnas.1518377113.

112. Naci, L., Sinai, L., and Owen, A.M. (2017). Detecting and interpreting conscious experiences in behaviorally non-responsive patients. NeuroImage *145*, 304–313. 10.1016/j.neuroimage.2015.11.059.

113. Naci, L., Cusack, R., Anello, M., and Owen, A.M. (2014). A common neural code for similar conscious experiences in different individuals. Proceedings of the National Academy of Sciences of the United States of America *111*, 14277–14282. 10.1073/pnas.1407007111.

114. Lee, M., Sanz, L.R.D., Barra, A., Wolff, A., Nieminen, J.O., Boly, M., Rosanova, M., Casarotto, S., Bodart, O., Annen, J., et al. (2022). Quantifying arousal and awareness in altered states of consciousness using interpretable deep learning. Nature Communications *13*, 1–14. 10.1038/s41467-022-28451-0.

115. Ferrarelli, F., Massimini, M., Sarasso, S., Casali, A., Riedner, B.A., Angelini, G., Tononi, G., and Pearce, R.A. (2010). Breakdown in cortical effective connectivity during midazolam-induced loss of consciousness. Proceedings of the National Academy of Sciences *107*, 2681–2686. 10.1073/pnas.0913008107.

116. Bodart, O., Gosseries, O., Wannez, S., Thibaut, A., Annen, J., Boly, M., Rosanova, M., Casali, A.G., Casarotto, S., Tononi, G., et al. (2017). Measures of metabolism and complexity in the brain of patients with disorders of consciousness. Neuroimage Clin *14*, 354–362. 10.1016/j.nicl.2017.02.002.

117. Casali, A.G., Gosseries, O., Rosanova, M., Boly, M., Sarasso, S., Casali, K.R., Casarotto, S., Bruno, M.-A., Laureys, S., Tononi, G., et al. (2013). A Theoretically Based Index of Consciousness Independent of Sensory Processing and Behavior. In Science translational medicine, pp. 1–10.

118. Casarotto, S., Comanducci, A., Rosanova, M., Sarasso, S., Fecchio, M., Napolitani, M., Pigorini, A., Casali, A.G., Trimarchi, P.D., Boly, M., et al. (2016). Stratification of Unresponsive Patients by an Independently Validated Index of Brain Complexity. Ann Neurol *80*, 718–729. 10.1002/ana.24779.

119. Sarasso, S., Boly, M., Napolitani, M., Gosseries, O., Charland-Verville, V., Casarotto, S., Rosanova, M., Casali, A.G., Brichant, J.F., Boveroux, P., et al. (2015). Consciousness and complexity during unresponsiveness induced by propofol, xenon, and ketamine. Current Biology *25*, 3099–3105. 10.1016/j.cub.2015.10.014.

120. Shine, J.M., Bissett, P.G., Bell, P.T., Koyejo, O., Balsters, J.H., Gorgolewski, K.J., Moodie, C.A., and Poldrack, R.A. (2016). The Dynamics of Functional Brain Networks: Integrated Network States during Cognitive Task Performance. Neuron *92*, 544–554. 10.1016/j.neuron.2016.09.018.

121. Zamani Esfahlani, F., Jo, Y., Faskowitz, J., Byrge, L., Kennedy, D.P., Sporns, O., and Betzel, R.F. (2020). High-amplitude cofluctuations in cortical activity drive functional connectivity. Proceedings of the National Academy of Sciences of the United States of America *117*, 28393–28401. 10.1073/pnas.2005531117.

122. Faskowitz, J., Zamani Esfahlani, F., Jo, Y., Sporns, O., and Betzel, R.F. Edge-centric functional network representations of human cerebral cortex reveal overlapping system-level architecture. Nature Neuroscience *23*, 1644–1654. 10.1038/s41593-020-00719-y.

123. Lurie, D.J., Kessler, D., Bassett, D.S., Betzel, R.F., Breakspear, M., Kheilholz, S., Kucyi, A., Liégeois, R., Lindquist, M.A., McIntosh, A.R., et al. (2020). Questions and controversies in the study of time-varying functional connectivity in resting fMRI. Network Neuroscience *4*, 30–69. 10.1162/netn_a_00116.

124. Cabral, J., Fernandes, F.F., and Shemesh, N. (2023). Intrinsic macroscale oscillatory modes driving long range functional connectivity in female rat brains detected by ultrafast fMRI. Nat Commun *14*, 375. 10.1038/s41467-023-36025-x.

125. Raut, R.V., Snyder, A.Z., Mitra, A., Yellin, D., Fujii, N., Malach, R., and Raichle, M.E. (2021). Global waves synchronize the brain's functional systems with fluctuating arousal. Science Advances *7*, eabf2709. 10.1126/SCIADV.ABF2709.

126. Vidaurre, D., Smith, S.M., and Woolrich, M.W. (2017). Brain network dynamics are hierarchically organized in time. Proceedings of the National Academy of Sciences of the United States of America *114*, 12827–12832. 10.1073/pnas.1705120114.

127. Atasoy, S., Deco, G., Kringelbach, M.L., and Pearson, J. (2018). Harmonic Brain Modes: A Unifying Framework for Linking Space and Time in Brain Dynamics. Neuroscientist *24*, 277–293. 10.1177/1073858417728032.

128. Demertzi, A., Tagliazucchi, E., Dehaene, S., Deco, G., Barttfeld, P., Raimondo, F., Martial, C., Fernández-Espejo, D., Rohaut, B., Voss, H.U., et al. (2019). Human consciousness is supported by dynamic complex patterns of brain signal coordination. Science Advances *5*, 1–12. 10.1126/sciadv.aat7603.

129. Gutierrez-Barragan, D., Singh, N.A., Alvino, F.G., Coletta, L., Rocchi, F., De Guzman, E., Galbusera, A., Uboldi, M., Panzeri, S., and Gozzi, A. (2021). Unique spatiotemporal fMRI dynamics in the awake mouse brain. Current biology *32*, 1–14. 10.1016/J.CUB.2021.12.015.

130. Luppi, A.I., Carhart-Harris, R.L., Roseman, L., Pappas, I., Menon, D.K., and Stamatakis, E.A. (2021). LSD alters dynamic integration and segregation in the human brain. NeuroImage *227*, 117653. 10.1016/j.neuroimage.2020.117653.

131. Luppi, A.I., Golkowski, D., Ranft, A., Ilg, R., Jordan, D., Menon, D.K., and Stamatakis, E.A. (2021). Brain network integration dynamics are associated with loss and recovery of

consciousness induced by sevoflurane. Human Brain Mapping *42*, 2802–2822. 10.1002/hbm.25405.

132. Lord, L.D., Expert, P., Atasoy, S., Roseman, L., Rapuano, K., Lambiotte, R., Nutt, D.J., Deco, G., Carhart-Harris, R.L., Kringelbach, M.L., et al. (2019). Dynamical exploration of the repertoire of brain networks at rest is modulated by psilocybin. NeuroImage *199*, 127–142. 10.1016/j.neuroimage.2019.05.060.

133. Barttfeld, P., Uhrig, L., Sitt, J.D., Sigman, M., Jarraya, B., and Dehaene, S. (2015). Signature of consciousness in the dynamics of resting-state brain activity. Proceedings of the National Academy of Sciences *112*, 887–892. 10.1073/pnas.1418031112.

134. Uhrig, L., Sitt, J.D., Jacob, A., Tasserie, J., Barttfeld, P., Dupont, M., Dehaene, S., and Jarraya, B. (2018). Resting-state Dynamics as a Cortical Signature of Anesthesia in Monkeys. Anesthesiology *129*, 942–958. 10.1097/ALN.0000000000002336.

135. Stevner, A.B.A., Vidaurre, D., Cabral, J., Rapuano, K., Nielsen, S.F.V., Tagliazucchi, E., Laufs, H., Vuust, P., Deco, G., Woolrich, M.W., et al. (2019). Discovery of key whole-brain transitions and dynamics during human wakefulness and non-REM sleep. Nature Communications *10*. 10.1038/s41467-019-08934-3.

136. Bayne, T., Seth, A.K., and Massimini, M. (2020). Are There Islands of Awareness? Trends in Neurosciences *43*, 6–16. 10.1016/j.tins.2019.11.003.

137. Connor, D., and Shanahan, M. (2007). A simulated global neuronal workspace with stochastic wiring. AI and Consciousness: Theoretical Foundations and Current Approaches, 43–48.

138. Shanahan, M. (2006). A cognitive architecture that combines internal simulation with a global workspace. Consciousness and Cognition *15*, 433–449. 10.1016/j.concog.2005.11.005.

139. Langdon, A., Botvinick, M., Nakahara, H., Tanaka, K., Matsumoto, M., and Kanai, R. (2022). Meta-learning, social cognition and consciousness in brains and machines. Neural Networks *145*, 80–89. 10.1016/J.NEUNET.2021.10.004.

140. VanRullen, R., and Kanai, R. (2021). Deep learning and the Global Workspace Theory. Trends in Neurosciences. 10.1016/j.tins.2021.04.005.

141. Proca, A.M., Rosas, F.E., Luppi, A.I., Bor, D., Crosby, M., and Mediano, P.A.M. (2022). Synergistic information supports modality integration and flexible learning in neural networks solving multiple tasks.

142. Luppi, A.I., Mediano, P.A.M., Rosas, F.E., Allanson, J., Pickard, J.D., Williams, G.B., Craig, M.M., Finoia, P., Peattie, A.R.D., Coppola, P., et al. (2022). Whole-brain modelling identifies distinct but convergent paths to unconsciousness in anaesthesia and disorders of consciousness. Communications biology *5*, 384. 10.1038/S42003-022-03330-Y.

143. Naci, L., Haugg, A., MacDonald, A., Anello, M., Houldin, E., Naqshbandi, S., Gonzalez-Lara, L.E., Arango, M., Harle, C., Cusack, R., et al. (2018). Functional diversity of brain networks supports consciousness and verbal intelligence. Scientific Reports *8*, 1–15. 10.1038/s41598-018-31525-z.

144. Kandeepan, S., Rudas, J., Gomez, F., Stojanoski, B., Valluri, S., Owen, A.M., Naci, L., Nichols, E.S., and Soddu, A. (2020). Modeling an auditory stimulated brain under altered states of consciousness using the generalized ising model. NeuroImage *223*, 117367. 10.1016/j.neuroimage.2020.117367.

145. Varley, T.F., Luppi, A.I., Pappas, I., Naci, L., Adapa, R., Owen, A.M., Menon, D.K., and Stamatakis, E.A. (2020). Consciousness & Brain Functional Complexity in Propofol Anaesthesia. Scientific Reports *10*, 1–13. 10.1038/s41598-020-57695-3.

146. Varley, T.F., Craig, M.M., Adapa, R., Finoia, P., Williams, G., Allanson, J., Pickard, J., Menon, D.K., and Stamatakis, E.A. (2020). Fractal dimension of cortical functional connectivity networks & severity of disorders of consciousness. PLoS ONE *15*, 1–20. 10.1371/journal.pone.0223812.

147. Whitfield-Gabrieli, S., and Nieto-Castanon, A. (2012). Conn: A Functional Connectivity Toolbox for Correlated and Anticorrelated Brain Networks. Brain Connectivity *2*, 125–141. 10.1089/brain.2012.0073.

148. van Dijk, K.R.A., Sabuncu, M.R., and Buckner, R.L. (2012). The influence of head motion on intrinsic functional connectivity MRI. NeuroImage *59*, 431–438. 10.1016/j.neuroimage.2011.07.044.

149. Power, J.D., Barnes, K.A., Snyder, A.Z., Schlaggar, B.L., and Petersen, S.E. (2012). Spurious but systematic correlations in functional connectivity MRI networks arise from subject motion. NeuroImage *59*, 2142–2154. 10.1016/j.neuroimage.2011.10.018.

150. Behzadi Y, Restom K, Liau J, and Liu TT (2007). A component based noise correction method (CompCor) for BOLD and perfusion based fMRI. NeuroImage *37*, 90–101.

151. Power, J.D., Mitra, A., Laumann, T.O., Snyder, A.Z., Schlaggar, B.L., and Petersen, S.E. (2014). Methods to detect, characterize, and remove motion artifact in resting state fMRI. NeuroImage *84*, 320–341. 10.1016/j.neuroimage.2013.08.048.

152. Lydon-Staley, D.M., Ciric, R., Satterthwaite, T.D., and Bassett, D.S. (2019). Evaluation of confound regression strategies for the mitigation of micromovement artifact in studies of dynamic resting-state functional connectivity and multilayer network modularity. Network Neuroscience *3*, 427–454. 10.1162/netn_a_00071.

153. Andellini, M., Cannatà, V., Gazzellini, S., Bernardi, B., and Napolitano, A. (2015). Test-retest reliability of graph metrics of resting state MRI functional brain networks: A review. Journal of Neuroscience Methods *253*, 183–192. 10.1016/j.jneumeth.2015.05.020.

154. Murphy, K., and Fox, M.D. (2017). Towards a consensus regarding global signal regression for resting state functional connectivity MRI. NeuroImage *154*, 169–173. 10.1016/j.neuroimage.2016.11.052.

155. Tanabe, S., Huang, Z., Zhang, J., Chen, Y., Fogel, S., Doyon, J., Wu, J., Xu, J., Zhang, J., Qin, P., et al. (2020). Altered Global Brain Signal during Physiologic, Pharmacologic, and Pathologic States of Unconsciousness in Humans and Rats. Anesthesiology, 1392–1406. 10.1097/ALN.0000000000003197.

156. Cover, T.M., and Thomas, J.A. (2005). Elements of Information Theory (Wiley-Interscience) 10.1002/047174882X.

157. Barrett, A.B. (2015). Exploration of synergistic and redundant information sharing in static and dynamical Gaussian systems. Physical Review E *91*, 52802. 10.1103/PhysRevE.91.052802.

158. Schulz, M.A., Yeo, B.T.T., Vogelstein, J.T., Mourao-Miranada, J., Kather, J.N., Kording, K., Richards, B., and Bzdok, D. (2020). Different scaling of linear models and deep learning in UK Biobank brain images vs. machine-learning datasets. Nature Communications *11*. 10.1101/757054.

159. Nozari, E., Stiso, J., Caciagli, L., Cornblath, E.J., He, X., Bertolero, M.A., Mahadevan, A.S., Pappas, G.J., and Bassett, D.S. (2020). Is the brain macroscopically linear? A system identification of resting state dynamics. bioRxiv. 10.1101/2020.12.21.423856.

160. Mediano, P.A.M., Rosas, F.E., Luppi, A.I., Jensen, H.J., Seth, A.K., Barrett, A.B., Carhart-Harris, R.L., and Bor, D. (2022). Greater than the parts: a review of the information decomposition approach to causal emergence. Philosophical transactions. Series A, Mathematical, physical, and engineering sciences *380*. 10.1098/RSTA.2021.0246.

161. Lizier, J.T. (2014). JIDT: An Information-Theoretic Toolkit for Studying the Dynamics of Complex Systems. Frontiers in Robotics and AI *1*, 1–37. 10.3389/frobt.2014.00011.

162. Mediano, P.A.M., Seth, A.K., and Barrett, A.B. (2019). Measuring integrated information: Comparison of candidate measures in theory and simulation. Entropy *21*. 10.3390/e21010017.

163. Tegmark, M. (2016). Improved Measures of Integrated Information. PLoS Computational Biology *12*. 10.1371/journal.pcbi.1005123.

164. Barrett, A.B., and Seth, A.K. (2011). Practical Measures of Integrated Information for Time-Series Data. PLoS Comput Biol *7*, 1001052. 10.1371/journal.pcbi.1001052.

165. Oizumi, M., Tsuchiya, N., and Amari, S.I. (2016). Unified framework for information integration based on information geometry. Proceedings of the National Academy of Sciences of the United States of America *113*, 14817–14822. 10.1073/pnas.1603583113.

166. Barrett, A.B., and Mediano, P.A.M. (2019). The phi measure of integrated information is not well-defined for general physical systems. Journal of Consciousness Studies *26*, 11–20.

167. Barbosa, L.S., Marshall, W., Albantakis, L., and Tononi, G. (2021). Mechanism Integrated Information. Entropy *23*, 362. 10.3390/e23030362.

168. Rubinov, M., and Sporns, O. (2011). Weight-conserving characterization of complex functional brain networks. NeuroImage *56*, 2068–2079. 10.1016/j.neuroimage.2011.03.069.

169. Lehmann, E.L., and Romano, J.P. (2005). Testing Statistical Hypotheses Third Edition With 6 Illustrations.